regulate transcriptional memory in *Drosophila*.

Hyperacetylation of histone H3 and H4 by histone acetyltransferases was suggested to be associated with active chromatin (33). Recently, we and others have demonstrated that histone hyperacetylation of the Th2 cytokine gene loci occurs in developing Th2 cells in a Th2-specific and STAT6-dependent manner (34–36). We demonstrated an essential role for GATA3 in the Th2-specific hyperacetylation (34). We also generated a precise map of the Th2-specific histone hyperacetylation within the IL-13 and IL-4 gene loci and identified a 71-bp conserved GATA3 response element 1.6 kilobase pairs upstream of IL-13 locus exon 1. This histone hyperacetylation remodeling process could be a major target for the Th2 master transcription factor GATA3 to induce differentiation toward Th2 cells.

Histone hyperacetylation of another Th2 cytokine gene locus, IL-5, occurs in a Th2-specific STAT6- and GATA3-dependent manner with significantly different kinetics compared with that of the IL-4 and IL-13 genes (34). The direction of transcription of the IL-5 gene is opposite to that of IL-13 and IL-4. In addition, the RAD50 gene encoding a DNA repair enzyme is located between the IL-5 and IL-13 gene loci. A differential role for GATA3 in the regulation of promoter activity of the IL-5 gene from IL-4 has been suggested (37–39). These results encouraged us to explore possible novel molecular mechanisms that would govern histone hyperacetylation of the IL-5 gene locus.

In the present study we investigated histone hyperacetylation of the IL-5 gene locus in developing Th2 cells cultured with or without CD28 costimulation. A long range CD28-sensitive Th2-specific histone hyperacetylation was detected in the IL-5 and intergenic region of the IL-5 and RAD50 gene loci. The hyperacetylation was accompanied by CD28-sensitive intergenic transcripts and required high expression of GATA3. A molecular mechanism that governs Th2-specific histone hyperacetylation of the IL-5-gene associated nucleosomes will be discussed.

MATERIALS AND METHODS

Mice—C57BL/6 mice were purchased from SLC (Shizuoka, Japan). STAT6-deficient (KO) mice were kindly provided by Shizuo Akira (Osaka University, Osaka, Japan) (40). All mice used in this study were maintained under specific-pathogen-free conditions and were about 4 weeks old. Animal care was in accordance with the guidelines of Chiba University.

Immunofluorescent Staining and Flow Cytometry Analysis—In general, one million cells were stained with appropriate specific antibodies according to a standard method (41, 42). For intracellular staining, fluorescein isothiocyanate-conjugated anti-IFN-γ antibody (XMG1.2; Pharmingen), phosphatidylethanolamine-conjugated anti-IL-4 antibody (11B11; Pharmingen), and allophycocyanin-conjugated anti-IL-5 antibody (TRFK5; Pharmingen) were used. To detect intracellular IL-13, biotinylated polyclonal anti-IL-13 antibody (R&D Systems), and phosphatidylethanolamine-conjugated avidin were used. Flow cytometry analysis was performed on a FACScalibur (BD Biosciences), and results were analyzed by CELLQUEST software (BD Biosciences).

Cell Cultures and in Vitro T Cell Differentiation—Splenic CD4 T cells were stained with anti-CD4-fluorescein isothiocyanate and then purified using magnetic beads and an Auto-MACS sorter® (Miltenyi Biotec), yielding a purity of >98%. Enriched CD4 T cells (1.5×10^6) were stimulated for 2 days with immobilized anti-TCR mAb (H57-597, 3 μg/ml) and soluble anti-CD28 mAb (37.51, 3 μg/ml) in the presence of IL-2 (25 units/ml), IL-12 (100 units/ml), and anti-IL-4 mAb (11B11, 25% culture supernatant) for Th1-skewed conditions. For Th2-skewed conditions, cells were stimulated with immobilized anti-TCR mAb as above but in the presence of IL-2 (25 units/ml), IL-4 (100 units/ml), and anti-IFNγ mAb (R4.6A2, 25% culture supernatant). The cells were then transferred to new dishes and cultured for another 5 days in the presence of immobilized anti-TCR mAb, soluble anti-CD28 mAb, and the cytokines present in the initial culture. To enhance the generation of IL-5-producing cells, stimulation with anti-TCR and anti-CD28 mAbs was performed during the second culture for 5 days. This procedure is slightly different from that used in our previous report (16). Where indicated, wortmannin (Calbiochem) was added to the culture at the doses of 30 or 300 nM for the first 2 days. *In vitro* differentiation was then assessed by intracellular cytokine staining with anti-IL-4, anti-IL-5, anti-IL-13, and anti-IFNγ or by ELISA as described (42).

Chromatin Immunoprecipitation (ChIP) Assay—The ChIP assay was performed using histone H3 ChIP assay kits (17-245: Upstate Biotechnology) as described (34). Anti-GATA3 Ab (H-48: Santa Cruz Biotechnology) was used for precipitation. Where indicated, GFP-positive retrovirus-infected cells were sorted by flow cytometry and subjected to ChIP assay. Several primer sequences for ChIP assay were described previously (34, 42). The primer pairs newly generated are as follows: IL-5 1-F, 5′-$^{-109}$GATTGTTAGCAATTATTCATTTC^{-87}-3′; IL-5, 1-R, 5′-$^{+244}$GGTTAGGACAGCCTACCCTAC^{+224}-3′; IL-5 2-F, 5′-$^{+224}$GTAGGGTAGGCTGTCCTAACC^{+244}-3′; IL-5 2-R, 5′-$^{+646}$GATGCGGGCCATGAGCACATG^{+626}-3′; IL-5 3-F, 5′-$^{+626}$CATGTGCTCATGGCCCGCATC^{+646}-3′; IL-5 3-R, 5′-$^{+1135}$CAGGAGCTTGAGACCTAGAGAG^{+1112}-3′; IL-5 4-F, 5′-$^{+1112}$CTCTCTAGGTCTCAAGCTCCTG^{+1135}-3′; IL-5 4-R, 5′-$^{+1431}$CAACAGAGCTTATATCTCCAGC^{+1453}-3′; IL-5 5-F, 5′-$^{+1452}$GCTGGAGATATAAGCTCTGTTG^{+1431}-3′; IL-5 5-R, 5′-$^{+1795}$GAGAGGCACTAGGATGAAGAG^{+1775}-3′; IL-5 6-F, 5′-$^{+1776}$CTCTTCATCCTAGTGCCTCTC^{+1795}-3′; IL-5 6-R, 5′-$^{+2142}$CTTCAGGAACACCAGACACATAG^{+2120}-3′; IL-5 7-F, 5′-$^{+2142}$CAGATGGTTGTGAGCCAACCATCT^{+2120}-3′; IL-5 7-R, 5′-$^{+2856}$CAAGAAGCAAATAGATCAGACTG^{+2834}-3′; IL-5 8-F, 5′-$^{+2834}$CAGTCTGATCTATTTGCTTCTTG^{+2856}-3′; IL-5 8-R, 5′-$^{+3218}$CTTAAATTGTGAAGTCCTGTCAC^{+3196}-3′; IL-5 9-F, 5′-$^{+3519}$CAAGGCTTTGTGCATGTTACCAAC^{+3542}-3′; IL-5 9-R, 5′-$^{+3919}$CAGTCATGGCACAGTCTGATTC^{+3898}-3′; IL-5-RAD50 1-F, 5′-$^{-15107}$ACTTCACACTGTATGACAGTG^{-15087}-3′; IL-5-RAD50 1-R, 5′-$^{-14691}$CCTGGCTGTGAATGAATATTTGTC^{-14714}-3′; IL-5-RAD50 2-F, 5′-$^{-14336}$ACGCATTGCCCAAATCTTCAG^{-14316}-3′; IL-5-RAD50 2-R, 5′-$^{-13904}$GAAGACGGTAAGTCCTGAGGCG^{-13925}-3′; IL-5-RAD50 3-F, 5′-$^{-13695}$GAGGACCCAAAAGTTCCGAACACG^{-13672}-3′; IL-5-RAD50 3-R, 5′-$^{-13405}$TTCTAAAAGACAACAGCTACTCGT^{-13428}-3′; IL-5-RAD50 4-F, 5′-$^{-13558}$AGCAACCGTAAGCTCGCACATTCC^{-13535}-3′; IL-5-RAD50 4-R, 5′-$^{-13195}$GACTGCACCCCAGCCTACCCATGC^{-13218}-3′; IL-5-RAD50 5-F, 5′-$^{-13429}$ACGAGTAGCTGTTGTCTTTTAGAA^{-13405}-3′; IL-5-RAD50 5-R, 5′-$^{-13039}$TCACGTGATCAAGAGAAACTACTC^{-13062}-3′; IL-5-RAD50 6-F, 5′-$^{-13216}$GCATGGGTAGGCTGGGGTGCAGTC^{-13195}-3′; IL-5-RAD50 6-R, 5′-$^{-12840}$GACAATCTGCAAGAGCAAGTGCTC^{-12863}-3′; IL-5-RAD50 7-F, 5′-$^{-11453}$CGGAGGATAATTCTCCTTAAAAGG^{-11410}-3′; IL-5-RAD50 7-R, 5′-$^{-11067}$GACAAGGTCTCATTGTAGCTGTGG^{-11090}-3′; IL-5-RAD50 8-F, 5′-$^{-9305}$GCTACATAATGAGTAACCAGCTTG^{-9282}-3′; IL-5-RAD50 8-R, 5′-$^{-8922}$GAGCTGGTGCAGACCTTGTTGCCAC^{-8947}-3′; IL-5-RAD50 9-F, 5′-$^{-7140}$GAGCTGCAAGGTAAAAGGTTAGAATAG^{-7114}-3′; IL-5-RAD50 9-R, 5′-$^{-6761}$GAATCTTCAAGGATTGGTGACTATACC^{-6787}-3′; L-5-RAD50 10-F, 5′-$^{-3625}$GATTCAGGGAAACAATCTGTGGATG^{-3613}-3′; IL-5-RAD50 10-R, 5′-$^{-3300}$GGGTTTATGTGTTCACCATGGACC^{-3323}-3′; IL-5-RAD50 11-F, 5′-$^{-938}$CCTGCACTTTTTGTCATAGGAACC^{-915}-3′; IL-5-RAD50 11-R, 5′-$^{-555}$GTGGTGGTACACACCAGCAGATGTG^{-580}-3′; IL-5-RAD50 14-F, 5′-$^{+2172}$AGGCTGAGGCTGAGCTGCTCCATG^{+2195}-3′; IL-5-RAD50 14-R, 5′-$^{+3549}$TAACTCAGTTGGTAACATGCACAA^{+3526}-3′. The numbers indicate positions relative to the first nucleotide of the IL-5 exon 1, which is designated as +1. The primer pairs for IL-5-RAD50 12 and 13 in Fig. 6 are the same as those for IL-5 promoter and IL-5 intron, respectively.

ELISA—CD4 T cells were cultured for 7 days as described above and restimulated with immobilized anti-TCR mAb (H57-597, 3 μg/ml) for 8 h. The concentrations of IL-5, IL-4, IL-13, and IFNγ in the supernatant were determined by ELISA as described previously (42).

Retroviral Vectors and Infection—pMX-IRES-GFP plasmid was kindly provided by Toshio Kitamura (The University of Tokyo, Tokyo, Japan). The methods for the generation of virus supernatant and CD4 T cell infection were described previously (32). Infected cells were subjected to intracellular staining with anti-IL-4, anti-IL-5, and anti-IFNγ mAb or to cell sorting. A mutant of IκBα, IκBαM, was generated from the IκBα dominant-negative Vector (Mercury). cDNA for human IκBαM or human GATA3 were inserted into a multicloning site of pMX-IRES-GFP.

Immunoblot Analysis—Immunoblot analysis for GATA3, IκBα, and tubulin-α was performed as previously described (42). For IκBα, a rabbit polyclonal Ab (anti-IκBα; Cell Signaling Technology 9242) was used.

RT-PCR—Total RNA was isolated from cultured cells using the TRIzol reagent. Reverse transcription was carried out with Superscript II RT (Invitrogen). 3-Fold serial dilutions of template cDNA were performed. PCR reaction with specific primers was done as described previously (34). New primers used were GATA3 exon 1b forward, CTTTGCGGGATAGTTTAGCAA-3′, and GATA3 exon 1b reverse, 5′-GAA-

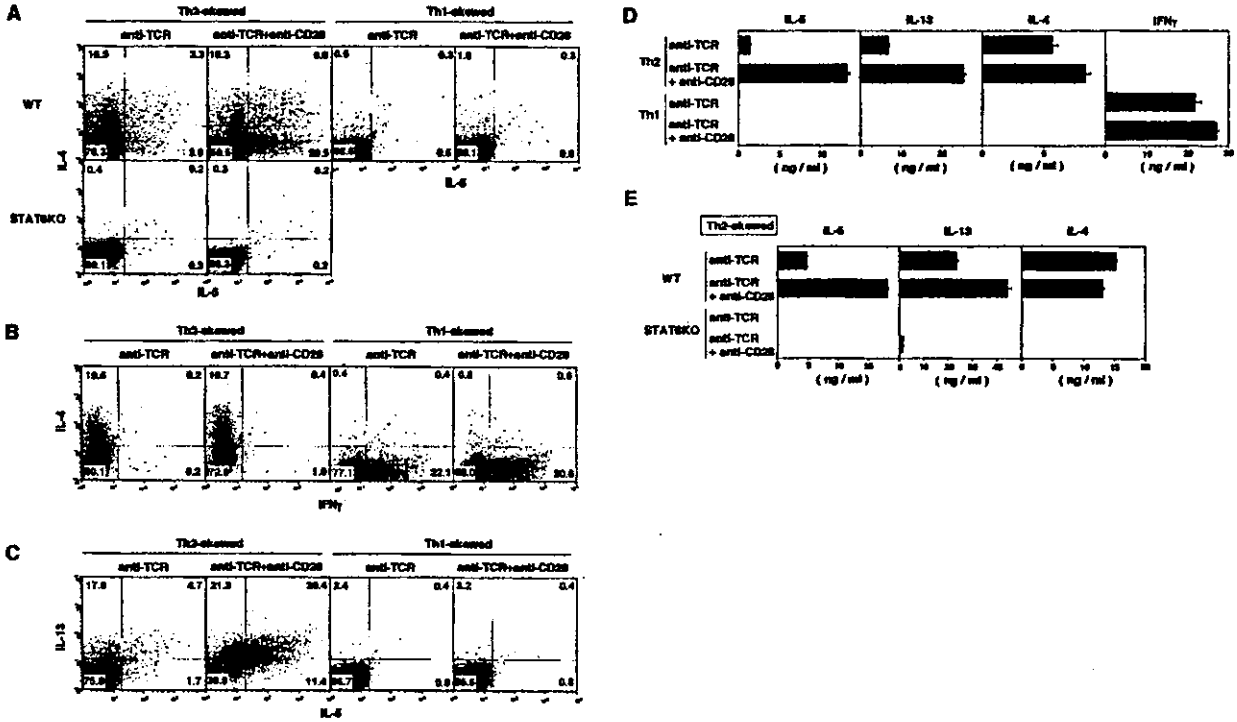

FIG. 1. **Costimulation with anti-CD28 mAb enhanced the generation of IL-5- and IL-13-producing cells.** *A*, *B*, and *C*, freshly prepared splenic CD4 T cells from B6 mice were cultured with immobilized anti-TCR mAb (H57-597, 3 μg/ml) in the presence of costimulation with agonistic anti-CD28 mAb (37.51, 3 μg/ml) under Th1- or Th2-skewed conditions for 7 days. The cultured cells were restimulated, and intracellular IL-5/IL-4, IFNγ/IL-4, and IL-5/IL-13 profiles were determined. The percentages of cells present in the each quadrant are shown. *D* and *E*, CD4 T cells from normal B6 or STAT6-KO mice were cultured under the conditions described above, and restimulation was done with anti-TCR mAb for 8 h. The amounts of IL-5, IL-13, IL-4, and IFNγ in the culture supernatant were measured by ELISA. *WT*, wild type.

CACTGAGCTGCCTGGCGCCGT. A detailed protocol for detection of intergenic transcripts was described previously (34). The primers used are the same as those used in ChIP assay.

RESULTS

Costimulation with Anti-CD28 mAb Enhances the Generation of IL-5- and IL-13-producing Cells—The aim of this study was to clarify the molecular mechanisms that control chromatin remodeling of the IL-5 gene locus during Th2 cell differentiation. We first assessed the role for CD28 costimulation in the generation of IL-5-producing Th2 cells. Freshly prepared CD4 T cells from young adult (4 weeks) B6 mice were cultured *in vitro* with immobilized anti-TCR in the presence of agonistic anti-CD28 mAbs (37.51) to effect stimulation. The IL-5/IL-4 profiles of CD4 T cells cultured under Th1- or Th2-skewed conditions are depicted in Fig. 1*A*. As can be seen, the generation of IL-5-producing cells (both $IL\text{-}5^+IL\text{-}4^-$ and $IL\text{-}5^+IL\text{-}4^+$ fractions) cultured under Th2-skewed conditions was greatly enhanced in the presence of CD28 costimulation. The increased generation of IL-4-producing cells was marginal under these culture conditions. IL-5-producing cells generated with CD28 costimulation were STAT6-dependent and not detected under Th1-skewed culture conditions. The generation of IFNγ-producing Th1 cells was moderately increased by the presence of CD28 costimulation (Fig. 1*B*). The levels of IL-13-producing cells were also increased by the presence of CD28 costimulation (Fig. 1*C*).

Concurrently, the amount of cytokines produced by developing Th2 cells cultured with CD28 costimulation was assessed by ELISA (Fig. 1, *D* and *E*). As expected, CD28 costimulation significantly enhanced the production of IL-5 and IL-13, whereas the effects on the production of IL-4 and IFNγ were marginal. The production of Th2 cytokines (IL-5, IL-13, and IL-4) was all STAT6-dependent regardless of the presence or absence of CD28 costimulation (Fig. 1*E*). Taken together these results suggest that the generation of IL-5- and IL-13-producing cells was Th2-specific, STAT6-dependent, and more sensitive to CD28 costimulation as compared with that of IL-4-producing cells.

Dynamics of Histone H3 Hyperacetylation of the IL-5 Gene Locus in Developing Th2 Cells Cultured with CD28 Costimulation—To clarify whether CD28 costimulation enhances histone hyperacetylation of the IL-5 gene locus during Th2 cell differentiation, we first examined the kinetics of acetylation of the IL-5 promoter, IL-4 promoter, and RAD50 promoter regions using a ChIP assay with anti-acetylhistone H3 Ab. Developing Th1 and Th2 cells cultured with CD28 costimulation were harvested 2, 3.5, 5, and 7 days after stimulation. The results of this analysis are presented as the relative band intensity of each group normalized with band intensity of the corresponding input DNA as shown in the *right panel* of Fig. 2. Two days after stimulation, low but significant levels of increase in acetylation occurred at all of the regions tested, and basically no difference between the three culture conditions was noted. However, as shown in Fig. 2*A*, the levels of histone acetylation associated with the IL-5 promoter increased significantly after cultivation for more than 3 days under Th2 skewed conditions, particularly in those cultures with CD28 costimulation. In contrast, the levels of histone hyperacetylation in the IL-4 promoter were increased day by day, and no significant difference was detected in the presence or absence of CD28 costimulation. The levels of histone hyperacetylation in the RAD50 gene promoter region were increased equivalently under these three culture conditions. These results suggest that histone hyperacetylation of the IL-5 gene locus is more sensitive to CD28

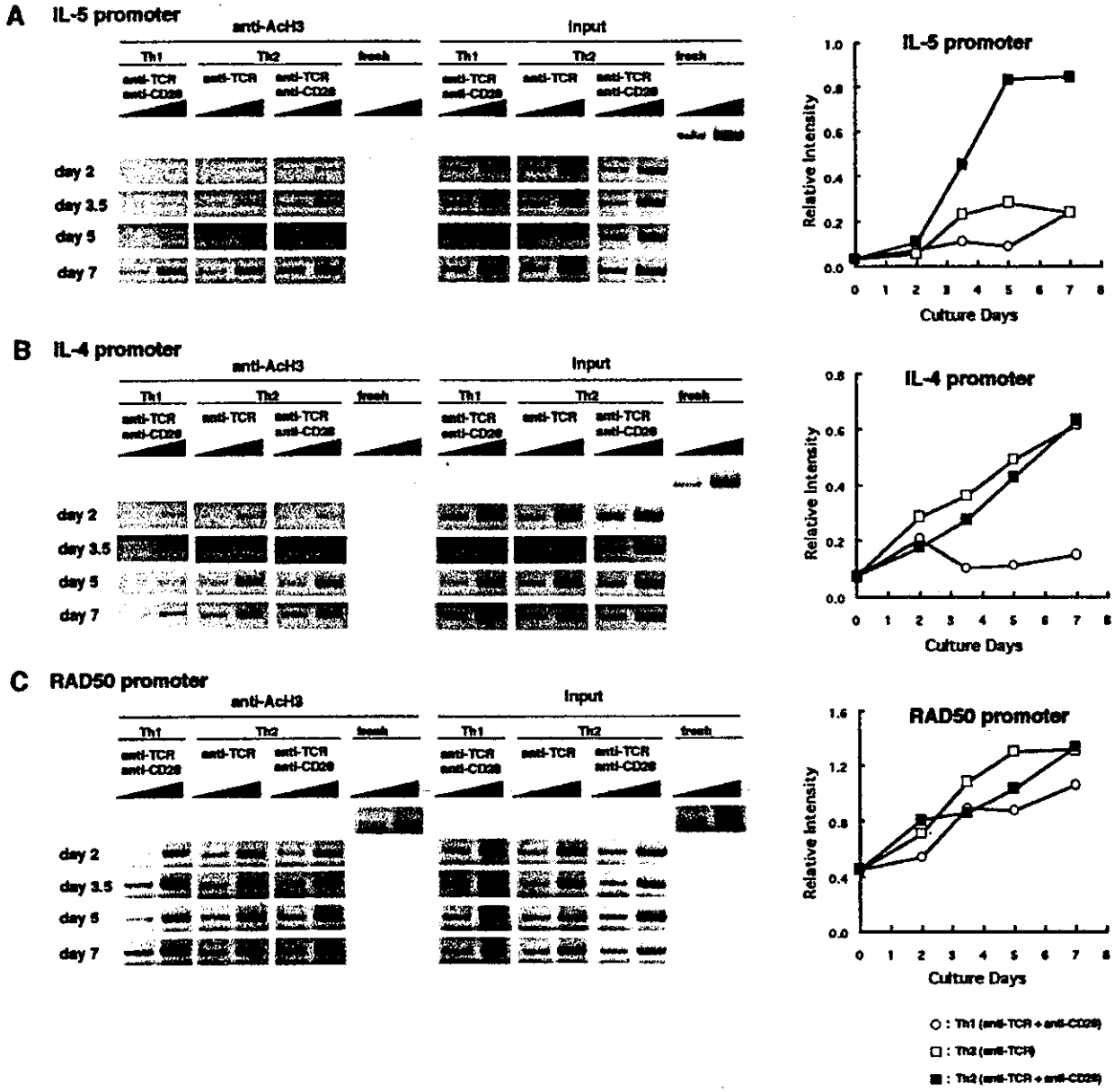

FIG. 2. **Induction of histone H3 hyperacetylation of IL-5, IL-4, and RAD50 gene loci in developing Th2 cells with CD28 costimulation.** Developing Th1 and Th2 cells cultured with immobilized anti-TCR mAb and CD28 costimulation were prepared 2, 3.5, 5, and 7 days after the stimulation. The acetylation status of histone H3 in the nucleosomes associated with the indicated regions was assessed by a ChIP assay with an anti-acetylated histone H3 antibody and specific primer pairs. Before immunoprecipitation for ChIP assay, aliquots of lysates (~6 × 10^2 cell equivalents) were separated for PCR to determine the relative levels of input DNA. 3-Fold serial dilutions were made with both the input DNA and immunoprecipitated DNA samples before PCR. Two independent experiments were performed, and similar results were obtained. Quantitative representations of the results are shown in the *right panels*. The intensities of the bands at the highest concentration were measured by densitometry, and relative intensities (anti-acetyl histone precipitates/input DNA ratio) for each primer pair were calculated.

costimulation than that of the IL-4 locus.

Enhanced Histone Hyperacetylation Induced with CD28 Costimulation Is Observed Only in the IL-5-associated Nucleosomes—Next, we examined the acetylation status of the DNA regions corresponding to IL-5 promoter, IL-5 intron, IL-13 intron, IL-4 promoter, CNS1, IL-4 V_A enhancer, RAD50 promoter, and IFNγ promoter. CNS1 and IL-4 V_A enhancer regions were previously described to contain regulatory elements or DNase I hypersensitive sites (28, 30). Histone hyperacetylation induced in these regions, except for two controls (RAD50 and IFNγ), occurred in a Th2-specific manner as reported previously (34). As can be seen in Fig. 3*A*, the levels of acetylation in the region of IL-5 promoter and IL-5 intron were significantly enhanced by the presence of CD28 costimulation. In contrast, those of other regions were all unaffected. The effect of CD28 costimulation on the histone hyperacetylation within the IL-5 gene loci was analyzed more precisely with a series of primer pairs within the IL-5 genes as shown in Fig. 3*B*. CD28 costimulation significantly enhanced the levels of histone hyperacetylation at all regions within the IL-5 genes tested (Fig. 3*C*).

Next, we assessed the STAT6 dependence of the CD28 costimulation-induced enhancement of the acetylation (Fig. 3*D*). Similar to other regions (IL-13 intron, IL-4 promoter,

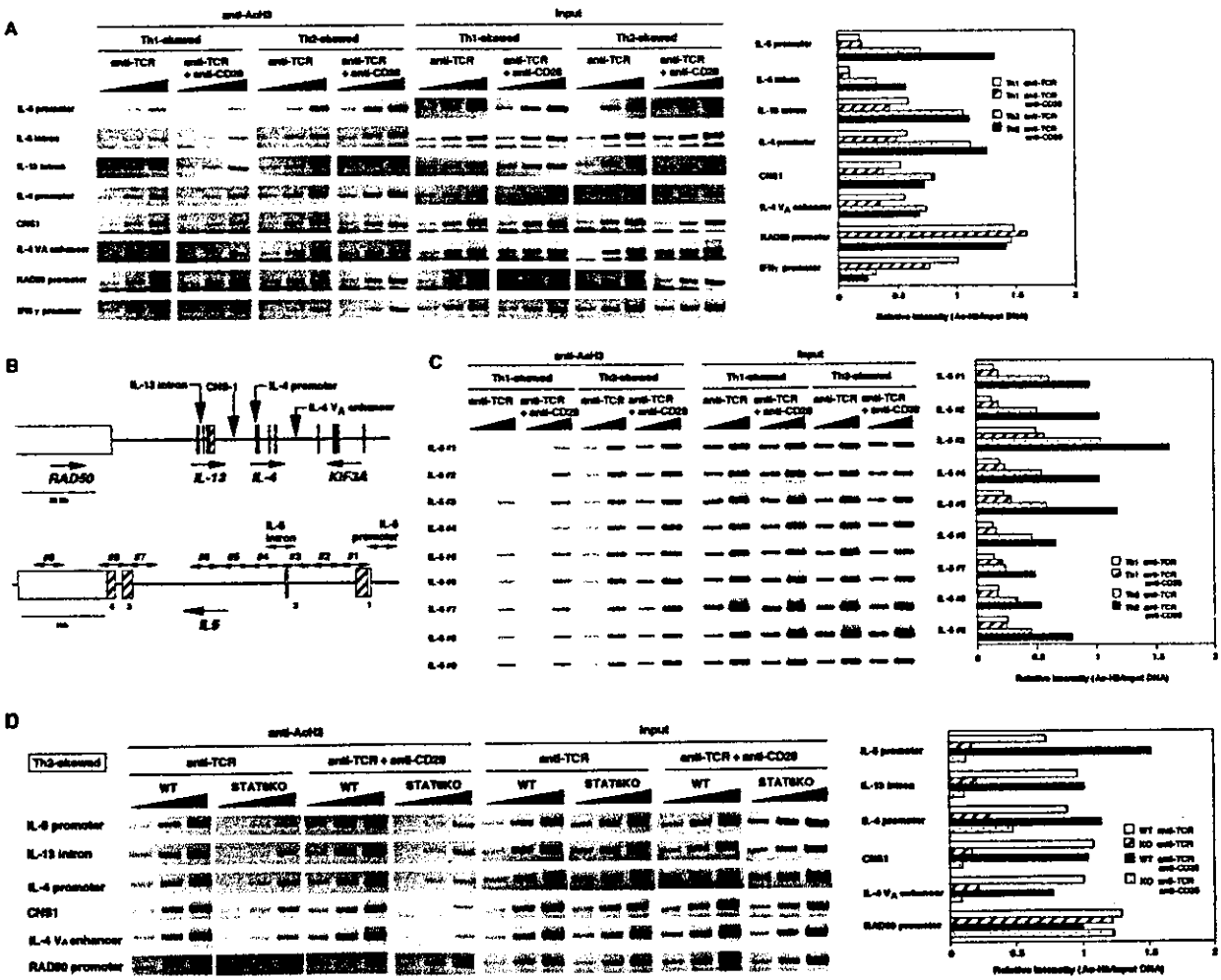

FIG. 3. **Hyperacetylation of histone H3 of the IL-5, IL-13, and IL-4 gene loci in developing Th2 cells cultured with CD28 costimulation.** *A*, developing Th1 and Th2 cells cultured with CD28 costimulation were prepared and subjected to ChIP assays with the indicated primer pairs. 3-Fold serial dilution series were made. The intensity of bands of the highest concentration was measured, and relative intensities are shown in the *right panel*. Similar results were obtained by measuring the bands of intermediate concentration. Three independent experiments with different T cell preparations were performed with similar results. *B*, schematic representation of the IL-5 gene locus and the IL-13 and IL-4 gene loci is shown with the location of the specific primers used in *panel A* and *C*. The location of the primer pairs used in *panel A* is as follows (5′ to 3′). IL-5 promoter F, −521 to −498; IL-5 promoter R, −76 to −101; IL-5 intron F, +857 to +883; IL-5 intron-R, +1214 to +1188. The numbers indicate positions relative to the first nucleotide of the IL-5 exon 1, which is designated as +1. IL-13 intron F, +142/+165; IL-13 intron R, +578 to +555; CNS1 F, +7554 to +7579; CNS1 R, +7767 to +7742. The numbers indicate positions relative to the first nucleotide of the IL-13 exon 1, which is designated as +1. IL-4 promoter F, −661 to −637; IL-4 promoter R, −164 to −187; IL-4 V_A enhancer F, +13234 to +13257; IL-4 V_A enhancer R, +13439 to +13416. The numbers indicate positions relative to the first nucleotide of the IL-4 exon 1, which is designated as +1. RAD50 promoter F, −242 to −217; RAD50 promoter R, −43 to −67. The numbers indicate positions relative to the first nucleotide of the RAD50 exon 1, which is designated as +1. IFNγ promoter F, −3372 to −3349; IFNγ promoter R, −3025 to −3048. The numbers indicate positions relative to the first nucleotide of the IFNγ exon 1, which is designated as +1. *kb*, kilobase. *C*, a ChIP assay with the indicated primer pairs within the IL-5 gene locus was done as in *panel A*. Three independent experiments were performed with similar results. *D*, a ChIP assay with STAT6-KO-developing Th2 cells was done as in *panel A*. Two independent experiments were performed with similar results.

CNS1, and IL-4 V_A enhancer), histone hyperacetylation of the IL-5 promoter locus was not induced in STAT6-KO T cell cultures even in the presence of CD28 costimulation. Thus, STAT6 is critical for the Th2-specific histone hyperacetylation of the IL-5 gene locus induced by anti-TCR stimulation and CD28 costimulation.

Enhanced Production of IL-5 and Histone Hyperacetylation of the IL-5 Gene Locus Induced by CD28 Costimulation Are Dependent on NF-κB Activation—CD28 costimulation is known to induce phosphatidylinositol 3-kinase activation and the subsequent activation of NF-κB. We tested the effect of wortmannin, a phosphatidylinositol 3-kinase inhibitor, on the CD28-induced enhancement of the generation of IL-5-producing cells (43). The generation of IL-5-producing cells in the culture with CD28 costimulation was decreased in the presence of wortmannin in a dose-dependent manner (Fig. 4*A*). In contrast, the generation of IL-4-producing cells was not affected at any doses of wortmannin tested. Concurrently, the effect of wortmannin on the production of cytokines was assessed by ELISA (Fig. 4*B*), and as expected, the enhanced production of IL-5 with CD28 costimulation was sensitive to wortmannin. IL-13 production was also slightly decreased; however, the levels of IL-4 were not changed by the presence of 30 to 300 nM wortmannin.

Next, we assessed the role for NF-κB activation in the CD28-induced enhancement of the generation of IL-5-producing cells and histone hyperacetylation of the IL-5 gene locus. A mutant form of IκBα (IκBαM), which inhibits the NF-κB activation (44), was inserted in an IRES-GFP retroviral construct, and the

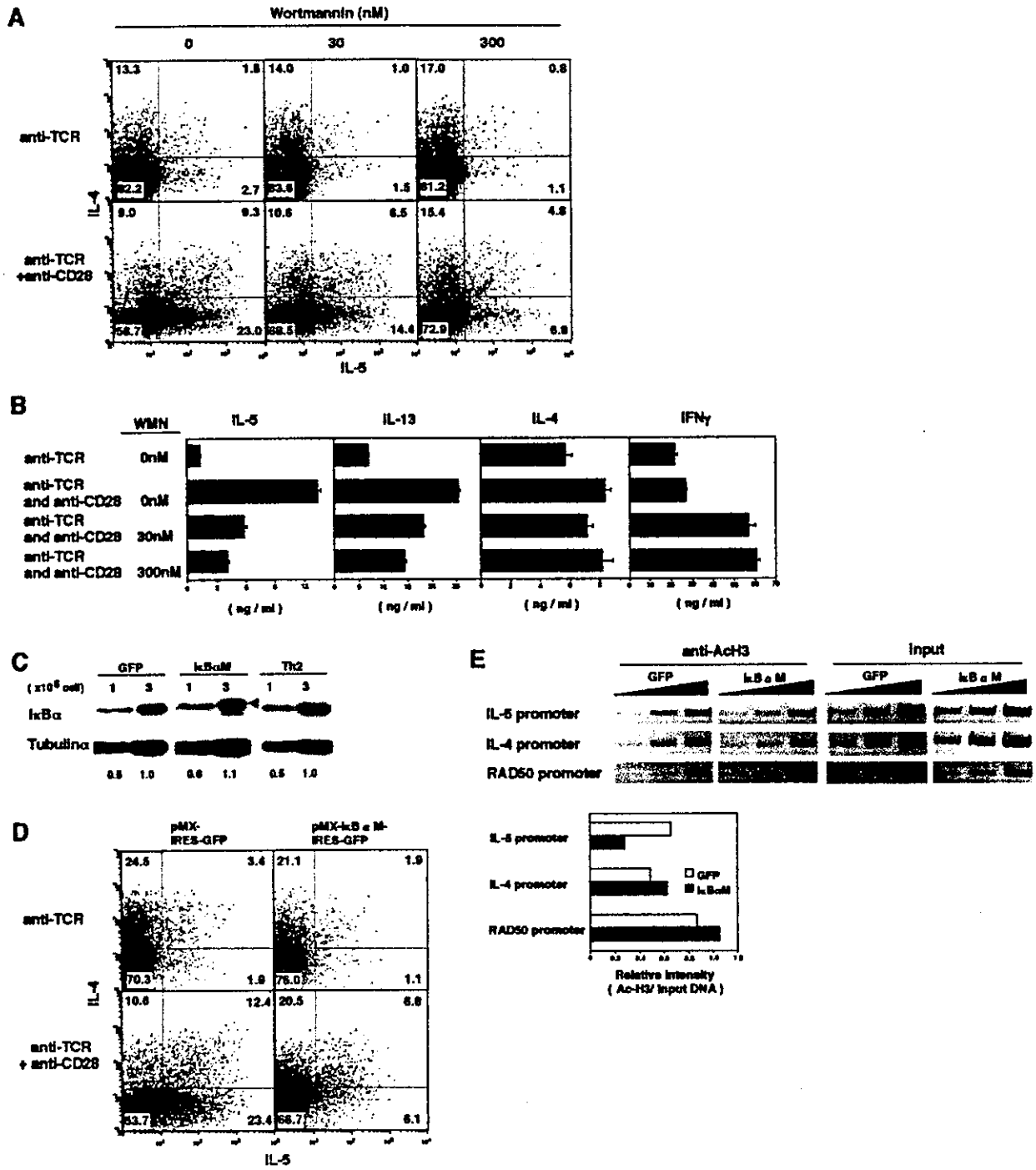

FIG. 4. **Enhanced production of IL-5 and histone hyperacetylation of the IL-5 gene locus induced by CD28 costimulation were dependent on NF-κB activation.** *A*, effect of wortmannin on the generation of IL-5-producing cells under Th2-skewed culture conditions with CD28 costimulation. CD4 T cells were cultured under the conditions described in Fig. 1 in the presence of the indicated doses of wortmannin. The intracellular IL-5/IL-4 profiles are shown. The *numbers* represent the percentages of the cells present in each quadrant. *B*, cytokine production profiles of the cells prepared under the same condition as described in *panel A* are shown. *C*, freshly prepared splenic CD4 T cells were stimulated with anti-TCR and anti-CD28 and infected with a retrovirus pMX-IRES-GFP (*GFP*) or pMX-IκBα-M-IRES-GFP encoding a mutant form of IκBα (*IκBαM*). Seven days after infection GFP^+ cells were sorted and subjected to immunoblotting with an anti-IκBα Ab that reacts with both wild type IκBα and IκBαM. The position of IκBαM is indicated by an *arrowhead*. Also non-infected Th2 cells (Th2) were included. Tubulin α was used as a loading control. *D*, freshly prepared splenic CD4 T cells were stimulated under the indicated conditions and infected with a retrovirus encoding a mutant form of IκBα (*IκBαM*) with EGFP. Seven days after infection, the cultured cells were restimulated, and intracellular IL-5/IL-4 profiles of electronically gated GFP positive populations were determined. The percentages of cells present in the each quadrant are shown. *E*, effect of ectopic expression of IκBαM on histone H3 hyperacetylation in IL-5, IL-4, and RAD5 gene loci. Retrovirus-infected CD4 T cells were prepared as described in *panel C*. One million GFP^+ infected cells were then collected by cell sorting and the acetylation status of histone H3 was determined by ChIP assay. Relative band intensities measured by densitometry are shown in the *right*. At least three independent experiments were done in each (*A–D*) with similar results.

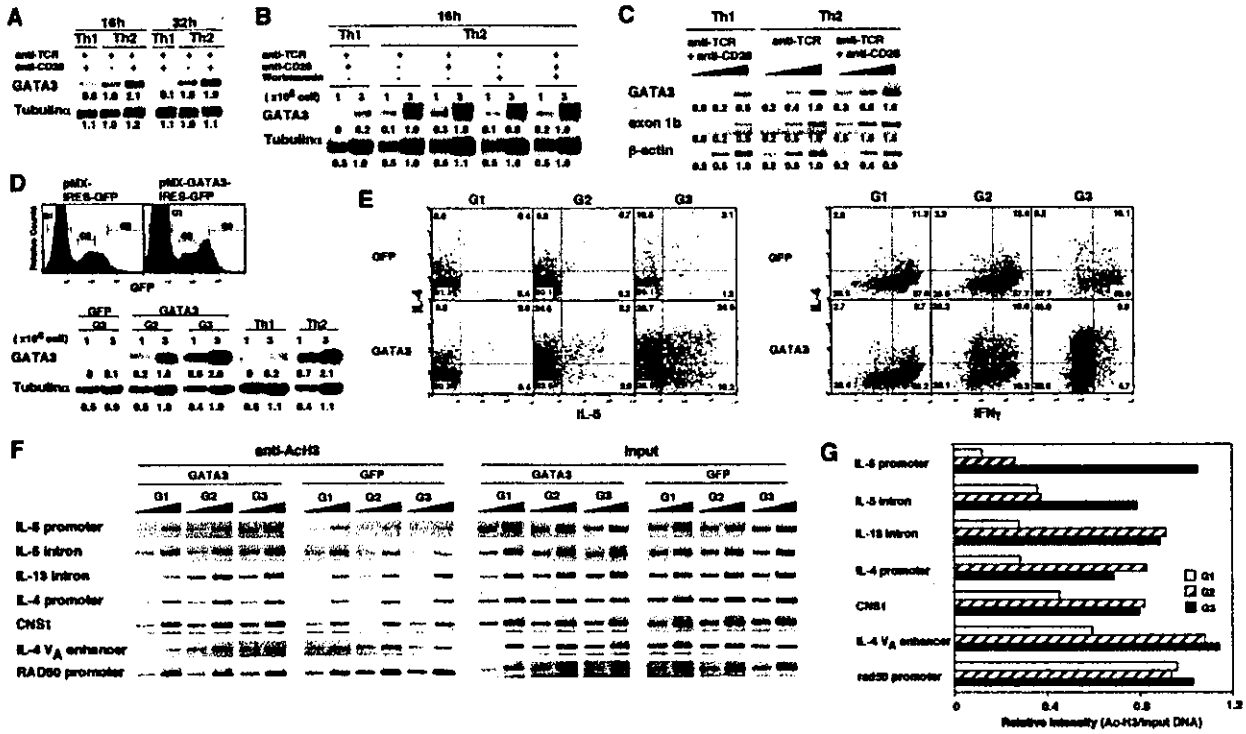

FIG. 5. **The generation of IL-5-producing cells and histone hyperacetylation of the IL-5 gene locus were highly dependent on the expression levels of GATA3.** *A*, freshly prepared CD4 T cells were cultured for 16 and 32 h under the conditions indicated, and the protein expression levels of GATA3 and tubulin α were determined by immunoblotting with specific mAbs. The lysates from 3×10^6 (*upper* for GATA3) and 0.3×10^6 (*lower* for tubulin α) cells were loaded per lane. The results are representative of three independent experiments. Arbitrary densitometric units are depicted under each band. *B*, the effect of wortmannin on the induction of GATA3 was assessed. The experiments as in *panel A* were done in the presence of wortmannin (300 ng/ml). *C*, freshly prepared CD4 T cells were cultured for 12 h under the conditions indicated, and total RNA was prepared. The transcription levels of GATA3, exon 1b of GATA3, and β-actin were determined by semiquantitative RT-PCR analysis with 3-fold serial dilution of template cDNA. Shown are the PCR product bands. Arbitrary densitometric units are indicated. Three independent experiments were done with similar results. *D*, freshly prepared CD4 T cells were stimulated under Th1-skewed conditions and were infected on day 2 with retrovirus encoding GATA3 bicistronically with EGFP (pMx-GATA3-IRES-GFP). The expression levels of GATA3 in the indicated populations sorted using GFP fluorescence were assessed by immunoblotting with anti-GATA3 Ab. Non-infected developing Th1 and Th2 cells were also included for comparison. Arbitrary densitometric units are indicated. *E*, three days after the infection as in *D*, the cells were restimulated, and intracellular IL-5/IL-4 and IFN-γ/IL-4 profiles of electronically gated GFP^- (gate G1), GFP^{low} (gate G2), and GFP^{high} (gate G3) populations were determined. The percentages of cells present in the each quadrant are shown. *F*, the cells present in the G1, G2, and G3 gate prepared as in *panel D* were sorted on day 5 by a cell sorter, and the acetylation status of histone H3 was determined by ChIP assay. *G*, relative band intensities (Ac-H3/Input DNA) of each group in *panel E* are shown. The results are representative of three independent experiments.

vectors were introduced into developing Th2 cells cultured with CD28 costimulation. The expression of the introduced IκBαM was confirmed by immunoblotting with an anti-IκBα Ab that reacts with both wild type IκBα and IκBαM (Fig. 4*C*). Substantial amounts of endogenous IκBα were detected in the GFP^+ population of mock pMX-IRES-GFP-infected cells (*GFP*) and non-infected Th2 cells (*Th2*). Also, substantial amounts of IκBαM were detected in the IκBαM-infected GFP^+ population (*IκBαM*). As previously reported, the *upper band*, indicated by an *arrowhead*, is IκBαM (45). The amount of endogenous IκBα in the IκBαM-infected cells was found to be reduced, probably as a result of the failure of NF-κB activation (46). The percentages of IL-5- and IL-4-producing cells in the GFP-positive infected cell population were determined (Fig. 4*D*). As can be seen, the numbers of IL-5-producing cells were decreased (12.4 ± 23.4 to 6.8 ± 6.1%) by the expression of IκBαM. Interestingly, the percentages of IL-4-producing cells were not significantly affected by IκBαM expression (10.6 ± 12.4 *versus* 20.5 ± 6.8%). The acetylation status of the IL-5 promoter, IL-4 promoter, and RAD50 promoter regions was assessed in the developing Th2 cells infected with IκBαM vector, and significant down-regulation of hyperacetylation in the IL-5-related nucleosomes was detected (Fig. 4*E*). Again, the introduction of IκBαM did not inhibit the acetylation levels of the IL-4- and RAD50-related nucleosomes, suggesting that NF-κB activation is preferentially involved in the process of hyperacetylation of the IL-5 gene locus.

The Generation of IL-5-producing Cells and Histone Hyperacetylation of the IL-5 Gene Locus Are Highly Dependent on the Expression Levels of GATA3—It is reported that the inhibition of NF-κB activity results in reduced GATA3 expression and Th2 cytokine production in developing but not committed Th2 cells (23). To examine the possible involvement of GATA3 in the CD28-induced enhancement of histone hyperacetylation of the IL-5 gene locus, we assessed the protein expression levels of GATA3 in developing Th2 cells cultured with CD28 costimulation. The GATA3 levels were clearly increased by the presence of CD28 costimulation at the 16- and 32-h time points (Fig. 5*A*). The increase was abrogated by the presence of wortmannin (Fig. 5*B*). Furthermore, the transcriptional levels of GATA3 as assessed by semiquantitative RT-PCR were significantly higher in the Th2 cell culture with CD28 costimulation (Fig. 5*C*). We also examined the transcriptional expression of GATA3 exon 1a and 1b (47). Although the expression of exon 1a transcript was undetectable in these developing Th2 cells, that of exon 1b was moderately enhanced in the presence of CD28 costimulation.

To examine the correlation between GATA3 expression and histone hyperacetylation of the IL-5 gene locus, we introduced

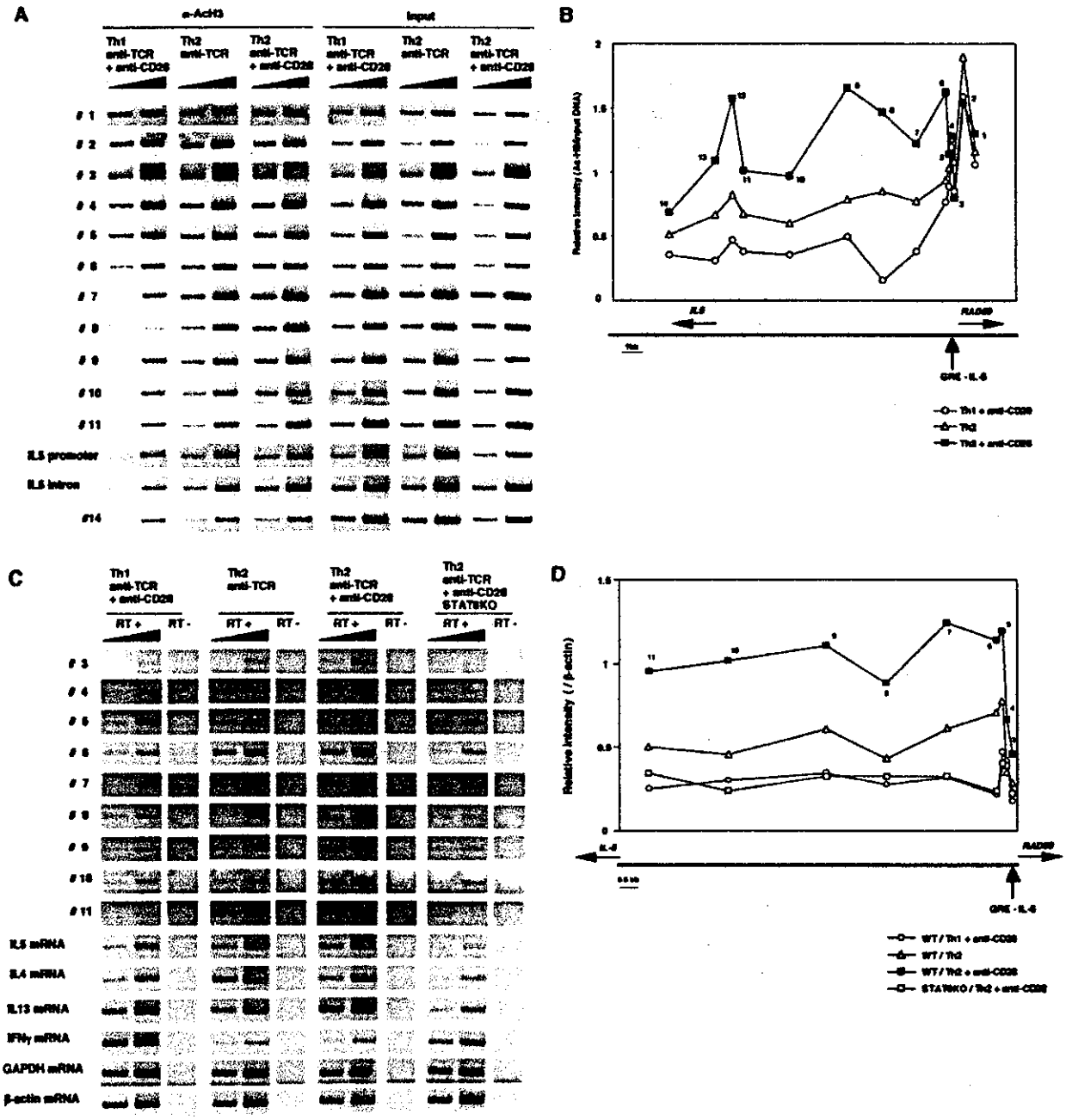

FIG. 6. **Long range histone hyperacetylation and intergenic transcripts in the intergenic region of the IL-5 and RAD50 loci in developing Th2 cells with CD28 costimulation.** *A* and *B*, splenic CD4 T cells were stimulated under the indicated conditions for 7 days, and a ChIP assay was performed. Shown are the PCR product bands for each primer pair (*A*) and the relative band intensities (*B*). The results are representative of three independent experiments. The location of GRE-IL-5 is indicated in *panel B*. *kb*, kilobase. *WT*, wild type. *C* and *D*, freshly prepared CD4 T cells from B6 and STAT6-KO mice were stimulated under the indicated conditions for 2 days and total RNA was prepared. RNA samples were treated with RNase free DNase I to eliminate any possible genomic DNA contamination, reverse-transcribed (RT^+), and then subjected to PCR with the indicated primer pairs. RT^- represents PCR without reverse transcription. *GAPDH*, glyceraldehyde-3-phosphate dehydrogenase. The numbers of the primer pairs are the same as those used in *panel A*. The intensity of bands of the highest concentration was measured, and relative intensities to the β-actin bands are shown in *panel D*. The results are representative of three independent experiments. *E* and *F*, the GATA3 introduced cells as in Fig. 5*D* were sorted (GFP^-, gate G1; GFP^{low}, gate G2; and GFP^{high}, gate G3), and subjected to ChIP assay with indicated primer pairs. The relative intensity (Ac-H3/Input DNA) of each band is shown in *panel F*. The results are representative of two independent experiments.

GATA3 into CD4 T cells stimulated under Th1-skewed conditions using a retroviral vector (pMX-IRES-EGFP) encoding GATA3 bicistronically with EGFP (pMX-GATA3-IRES-EGFP). The expression of GFP and GATA3 protein in the GATA3-infected T cells is depicted in Fig. 5. The expression levels of GATA3 in GFP^{high} (expressing high levels of GATA3, *G3*) population were ~2-fold as compared with those of GFP^{low} (expressing low levels of GATA3, *G2*) population and equivalent to those in Th2 cells. Next, the levels of IL-5- and IL-4-producing cells were compared between GFP^- (no GATA3 expression,

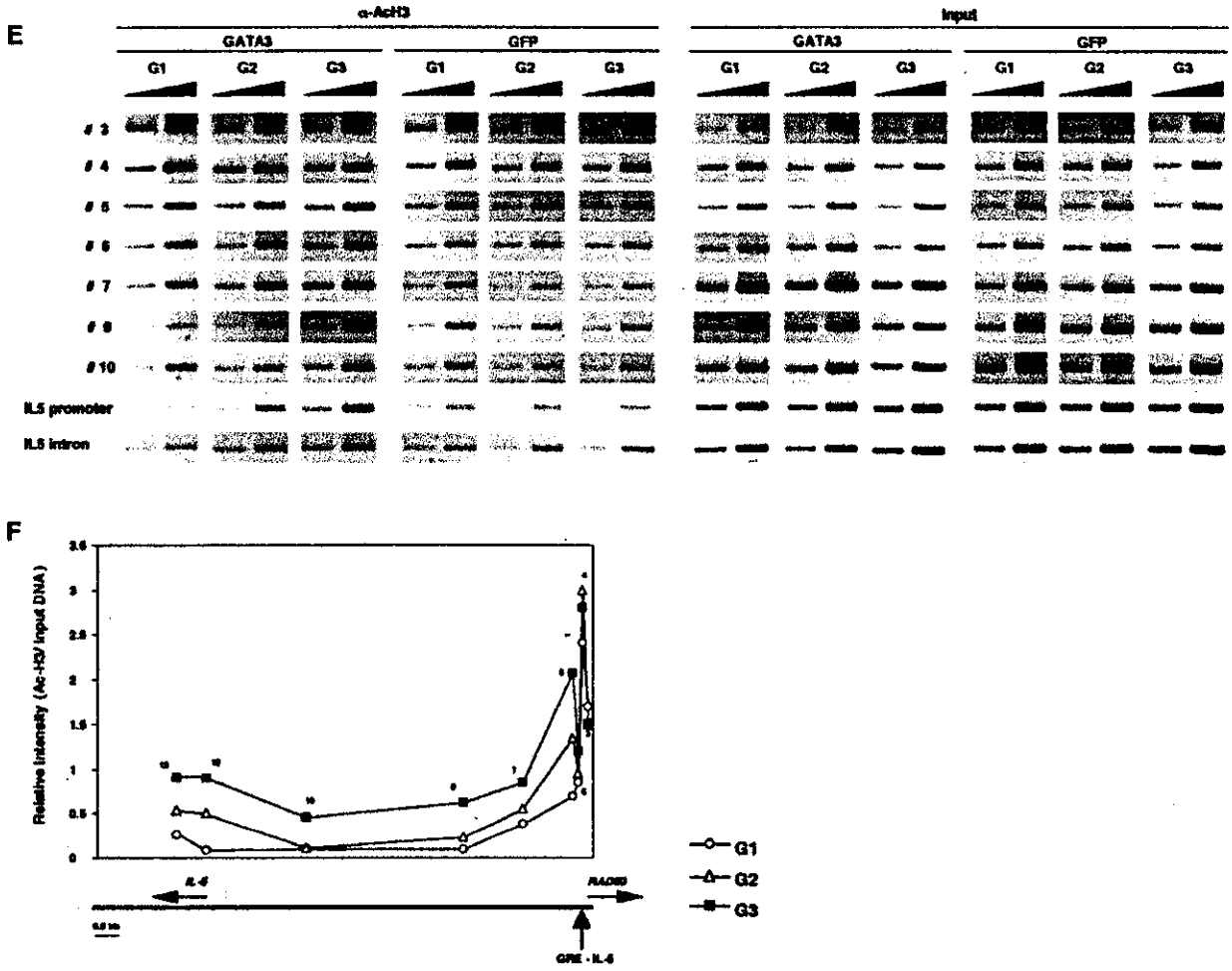

FIG. 6—*continued*

G1), GFP^{low}, and GFP^{high} populations. As shown in Fig. 5*E*, *left panels*, the generation of IL-5-producing cells was greatly increased in the fraction of high GATA3-expressing cells (G3) compared with that of low GATA3-expressing cells (G2) (24.5 ± 18.2 *versus* 8.2 ± 3.8%). The difference in the percentage of IL-5-producing cells was about 4-fold. In contrast, slight (~25%) increases in the generation of IL-4-producing cells were detected (G3, 28.7 ± 24.5%, *versus* G2, 34.6 ± 8.2%). As for the IFNγ-producing cells, a GATA3 dosage-dependent decrease was observed (Fig. 5*E*, *right*). No significant IFNγ/IL-5 double-producing cells were detected (data not shown).

To assess the acetylation status of histones in the GATA3-introduced developing T cells, GFP^{-}, GFP^{low}, and GFP^{high} cells prepared as above were purified by cell sorting and subjected to ChIP assay. Histone hyperacetylation of the Th2 cytokine loci (IL-5 promoter, IL-5 intron, IL-13 intron, IL-4 promoter, CNS1, IL-4 V_A enhancer) was significantly higher in GATA3-expressing cells (G2 and G3) compared with GATA3 non-expressing cells (G1) (Fig. 5*F*). The levels of histone hyperacetylation were increased concomitantly with the increase in the expression of GATA3 (compare G2 and G3) in the IL-5 gene locus (IL-5 promoter and IL-5 intron). No such increase was detected in the IL-4- and IL-13-related nucleosomes. These results suggest that the generation of IL-5-producing cells and histone hyperacetylation of the IL-5 gene locus are highly dependent on the expression levels of GATA3.

Long Range Th2-specific Hyperacetylation Detected in the Intergenic Region of the IL-5 and RAD50 Gene Loci Is Enhanced by the Presence of CD28 Costimulation—A series of primer pairs between the IL-5 and RAD50 loci were generated, and the acetylation status of the nucleosomes associated with IL-5 and RAD50 loci was analyzed. The actual band patterns of each ChIP assay (Fig. 6*A*) and the relative band intensities (Ac-H3/Input DNA) of the 14 selected primer pairs (Fig. 6*B*) are depicted. A long range Th2-specific hyperacetylation was observed from 400 bp upstream of the RAD50 exon 1 (corresponding to primer 5) to the end of IL-5 exon 4 (primer 14). The acetylation levels of all regions tested were significantly increased in the presence of CD28 costimulation. These results indicate that almost all histones from 400 bp upstream of the RAD50 exon 1 to the end of IL-5 exon 4 (primer 14) are selectively hyperacetylated under Th2-skewed culture conditions and are sensitive to CD28 costimulation.

Intergenic Transcription Is Detected throughout the Intergenic Region between the IL-5 and RAD50 Gene Loci—We demonstrated that the intergenic transcription throughout the IL-4 and IL-13 gene loci was accompanied by histone hyperacetylation (34). Thus, we examined the transcription of the intergenic region between the IL-5 and RAD50 gene loci. Interestingly, considerable amounts of transcripts were detected throughout the intergenic region, and the levels were significantly enhanced in the presence of CD28 costimulation (Fig. 6, *C* and *D*). In addition, we examined whether the intergenic transcripts were STAT6-dependent or not. STAT6-deficient CD4 T cells were used in paral-

lel. Only base-line levels of intergenic transcripts were detected. These results suggest that intergenic transcripts are induced throughout the intergenic region between the IL-5 and RAD50 gene loci in a Th2-specific and STAT6-dependent manner and are sensitive to CD28 costimulation.

CD28 Costimulation-sensitive Hyperacetylation in the Intergenic Region of the IL-5 and RAD50 Gene Loci Is Dependent on the Levels of GATA3 Expression—Next, we examined the correlation between the levels of GATA3 expression and histone hyperacetylation of the intergenic region. The retrovirus-induced GATA3-expressing cells shown in Fig. 5*D* were used to compare the acetylation status between GFP^- (no GATA3 expression, G1), GFP^{low} (expressing low levels of GATA3, G2), and GFP^{high} (expressing high levels of GATA3, G3) populations (Fig. 6*E*). The relative intensity (Ac-H3/input DNA) of each acetylation band of GATA3-introduced cells is shown in Fig. 6*F*. As expected, the levels of acetylation in the high GATA3-expressing cells (G3) were significantly higher than those of low and no GATA3-expressing cells (G2 and G1, respectively), suggesting that histone hyperacetylation of the intergenic region requires a high level expression of GATA3.

DISCUSSION

In this report we demonstrated that CD28 costimulation controls Th2-specific histone hyperacetylation of the IL-5 gene locus. CD28-mediated activation of NF-κB and the resulting enhancement of GATA3 induction appeared to be a mechanism by which histone hyperacetylation of the IL-5 gene locus was efficiently induced. This regulation was IL-5 gene-specific because the effect of CD28 costimulation was not observed in the acetylation of the IL-13 or IL-4 gene loci. A long range CD28-sensitive histone hyperacetylation with transcripts was detected in the IL-5 and intergenic region between the IL-5 and RAD50 gene.

The generation of IL-5- and IL-13-producing cells and the production of these cytokines were enhanced by CD28 costimulation of the differentiation culture (Fig. 1). A similar conclusion was drawn from the experiments with wortmannin (Fig. 4, *A* and *B*). As for histone hyperacetylation, however, CD28 costimulation affected only the IL-5 gene locus (Fig. 2 and 3). The transcription of IL-5 and IL-13 is known to be highly dependent on GATA3 as compared with that of IL-4 (11, 48, 49). An efficient transcription of IL-5 or IL-13 may require the enhanced levels of GATA3 that can be achieved by the presence of CD28-costimulation. Thus, it is possible that CD28 costimulation enhanced both histone hyperacetylation and transcription at the IL-5 gene locus but enhanced only transcription at the IL-13 gene. However, it would be unlikely that the enhancement of IL-5 and IL-13 production is mainly due to the effect on transcription, because we did not include anti-CD28 costimulation when the differentiated Th2 cells were restimulated. In fact, the production of IL-4 and IL-5 was only marginally increased when differentiated Th2 cells were restimulated with anti-TCR+anti-CD28.[2] This is consistent with the results reported previously (23).

NF-κB was reported to interact with histone acetyltransferases such as CREB-binding protein/p300 (50–52). In addition, NF-κB binding influenced the recruitment of SWI/SNF-type chromatin remodeling complexes in the granulocyte-macrophage colony-stimulating factor promoter in T cells (53). Thus, it is conceivable that CD28-induced NF-κB activation is involved directly in the acetylation of the IL-5 gene locus at the chromatin level. However, there is no NF-κB binding motif in the intergenic region of the IL-5 and RAD50 gene loci except for one in the promoter region of the IL-5 gene. Thus, it is most likely that the enhanced histone hyperacetylation of the IL-5 gene locus induced by the presence of CD28 costimulation is due to the enhanced expression of GATA3. NF-κB induces a wide variety of genes, such as cytokines (*e.g.* tumor necrosis factor-α and granulocyte-macrophage colony-stimulating factor), chemokines (*e.g.* MCP-1 (monocyte chemoattractant protein)), RANTES (regulated on activation normal T cell expressed and secreted), and eotaxin), and adhesion molecules (*e.g.* ICAM (intercellular adhesion molecule 1) and VCAM (vascular cell adhesion molecule 1) (54, 55). Thus, it is also possible that other genes regulated by NF-κB activation play critical roles in the histone hyperacetylation of the IL-5 gene locus; however, further investigation is required for addressing this issue.

We detected a long range histone hyperacetylation accompanying intergenic transcripts throughout the intergenic region of the IL-5 and RAD50 gene loci (Fig. 6). This is reminiscent of the GATA3-dependent hyperacetylation of the IL-13 and IL-4 gene loci (34, 42), suggesting that a similar molecular mechanism governs the acetylation events of both IL-13/IL-4 and IL-5 genes. The difference was the sensitivity to CD28 costimulation and the dependence on the levels of GATA3. Although the reason for the difference is not clear at this time, the nature of putative GATA response elements responsible for the IL-5 gene acetylation could be distinct from that of conserved GATA3 response element (34). There is 60% homology in the DNA sequence around the upstream region of human RAD50 gene compared with mouse, but we did not identify any conserved GATA binding motifs. However, there are several GATA binding motifs present in both mouse and human, suggesting a possible targeting of GATA3 to this region.

Hyperacetylation of the histone H3 (K9/14) and H4 (K5/8/12/16) is associated with transcriptionally active chromatin (33). However, acetylation of the histone H3-K9/14 does not always correlate with histone H4 acetylation (56). Furthermore, methylation of histone H3-K4 appears to be correlated with active chromatin (57). In the study we focused on the acetylation status of histone H3-K9/14. Thus, further analysis of histone H4 and histone H3-K4 methylation will be required to provide a more detailed view of the chromatin remodeling of the IL-5 gene locus.

In conclusion, we have demonstrated a possible molecular mechanism that controls histone hyperacetylation of the IL-5 gene locus. Characteristic features of chromatin remodeling of the IL-5 gene locus as compared with those of IL-13 and IL-4 were revealed to be the differential involvement of CD28 costimulation and sensitivity to the levels of GATA3 protein. This study is the first to provide evidence that CD28 costimulation controls chromatin remodeling during Th2 cell differentiation.

Acknowledgments—We are grateful to Dr. Ralph T. Kubo for helpful comments and constructive criticisms in the preparation of the manuscript. We also thank Kaoru Sugaya for excellent technical assistance.

REFERENCES

1. Mosmann, T. R., and Coffman, R. L. (1989) *Annu. Rev. Immunol.* **7**, 145–173
2. Seder, R. A., and Paul, W. E. (1994) *Annu. Rev. Immunol.* **12**, 635–673
3. Reiner, S. L., and Locksley, R. M. (1995) *Annu. Rev. Immunol.* **13**, 151–177
4. Abbas, A. K., Murphy, K. M., and Sher, A. (1996) *Nature* **383**, 787–793
5. Constant, S. L., and Bottomly, K. (1997) *Annu. Rev. Immunol.* **15**, 297–322
6. O'Garra, A. (2000) *Nature* **404**, 719–720
7. Yamashita, M., Hashimoto, K., Kimura, M., Kubo, M., Tada, T., and Nakayama, T. (1998) *Int. Immunol.* **10**, 577–591
8. Yamashita, M., Kimura, M., Kubo, M., Shimizu, C., Tada, T., Perlmutter, R. M., and Nakayama, T. (1999) *Proc. Natl. Acad. Sci. U. S. A.* **96**, 1024–1029
9. Yamashita, M., Katsumata, M., Iwashima, M., Kimura, M., Shimizu, C., Kamata, T., Shin, T., Seki, N., Suzuki, S., Taniguchi, M., and Nakayama, T. (2000) *J. Exp. Med.* **191**, 1869–1879
10. Rengarajan, J., Szabo, S. J., and Glimcher, L. H. (2000) *Immunol. Today* **21**, 479–483

[2] M. Inami, M. Yamashita, Y. Tenda, A. Hasegawa, M. Kimura, K. Hashimoto, N. Seki, M. Taniguchi, and T. Nakayama, unpublished observation.

11. Zhang, D. H., Cohn, L., Ray, P., Bottomly, K., and Ray, A. (1997) *J. Biol. Chem.* **272**, 21597–21603
12. Zheng, W., and Flavell, R. A. (1997) *Cell* **89**, 587–596
13. Ouyang, W., Ranganath, S. H., Weindel, K., Bhattacharya, D., Murphy, T. L., Sha, W. C., and Murphy, K. M. (1998) *Immunity* **9**, 745–755
14. Lee, H. J., Takemoto, N., Kurata, H., Kamogawa, Y., Miyatake, S., O'Garra, A., and Arai, N. (2000) *J. Exp. Med.* **192**, 105–115
15. Szabo, S. J., Kim, S. T., Costa, G. L., Zhang, X., Fathman, C. G., and Glimcher, L. H. (2000) *Cell* **100**, 655–669
16. Kubo, M., Yamashita, M., Abe, R., Tada, T., Okumura, K., Ransom, J. T., and Nakayama, T. (1999) *J. Immunol.* **163**, 2432–2442
17. Rulifson, I. C., Sperling, A. I., Fields, P. E., Fitch, F. W., and Bluestone, J. A. (1997) *J. Immunol.* **158**, 658–665
18. June, C. H., Bluestone, J. A., Nadler, L. M., and Thompson, C. B. (1994) *Immunol. Today* **15**, 321–331
19. Ward, S. G., June, C. H., and Olive, D. (1996) *Immunol. Today* **17**, 187–197
20. Kane, L. P., and Weiss, A. (2003) *Immunol. Rev.* **192**, 7–20
21. Lin, X., Cunningham, E. T., Jr., Mu, Y., Geleziunas, R., and Greene, W. C. (1999) *Immunity* **10**, 271–280
22. Rodriguez-Palmero, M., Hara, T., Thumbs, A., and Hunig, T. (1999) *Eur. J. Immunol.* **29**, 3914–3924
23. Das, J., Chen, C. H., Yang, L., Cohn, L., Ray, P., and Ray, A. (2001) *Nat. Immunol.* **2**, 45–50
24. Barnes, P. J., and Karin, M. (1997) *N. Engl. J. Med.* **336**, 1066–1071
25. Yang, L., Cohn, L., Zhang, D. H., Homer, R., Ray, A., and Ray, P. (1998) *J. Exp. Med.* **188**, 1739–1750
26. Donovan, C. E., Mark, D. A., He, H. Z., Liou, H. C., Kobzik, L., Wang, Y., De Sanctis, G. T., Perkins, D. L., and Finn, P. W. (1999) *J. Immunol.* **163**, 6827–6833
27. Agarwal, S., and Rao, A. (1998) *Curr. Opin. Immunol.* **10**, 345–352
28. Loots, G. G., Locksley, R. M., Blankespoor, C. M., Wang, Z. E., Miller, W., Rubin, E. M., and Frazer, K. A. (2000) *Science* **288**, 136–140
29. Mohrs, M., Blankespoor, C. M., Wang, Z. E., Loots, G. G., Afzal, V., Hadeiba, H., Shinkai, K., Rubin, E. M., and Locksley, R. M. (2001) *Nat. Immunol.* **2**, 842–847
30. Agarwal, S., Avni, O., and Rao, A. (2000) *Immunity* **12**, 643–652
31. Bird, J. J., Brown, D. R., Mullen, A. C., Moskowitz, N. H., Mahowald, M. A., Sider, J. R., Gajewski, T. F., Wang, C. R., and Reiner, S. L. (1998) *Immunity* **9**, 229–237
32. Kimura, M., Koseki, Y., Yamashita, M., Watanabe, N., Shimizu, C., Katsumoto, T., Kitamura, T., Taniguchi, M., Koseki, H., and Nakayama, T. (2001) *Immunity* **15**, 275–287
33. Strahl, B. D., and Allis, C. D. (2000) *Nature* **403**, 41–45
34. Yamashita, M., Ukai-Tadenuma, M., Kimura, M., Omori, M., Inami, M., Taniguchi, M., and Nakayama, T. (2002) *J. Biol. Chem.* **277**, 42399–42408
35. Avni, O., Lee, D., Macian, F., Szabo, S. J., Glimcher, L. H., and Rao, A. (2002) *Nat. Immunol.* **3**, 643–651
36. Fields, P. E., Kim, S. T., and Flavell, R. A. (2002) *J. Immunol.* **169**, 647–650
37. Lee, H. J., O'Garra, A., Arai, K., and Arai, N. (1998) *J. Immunol.* **160**, 2343–2352
38. Zhang, D. H., Yang, L., and Ray, A. (1998) *J. Immunol.* **161**, 3817–3821
39. Schwenger, G. T., Fournier, R., Kok, C. C., Mordvinov, V. A., Yeoman, D., and Sanderson, C. J. (2001) *J. Biol. Chem.* **276**, 48502–48509
40. Takeda, K., Tanaka, T., Shi, W., Matsumoto, M., Minami, M., Kashiwamura, S., Nakanishi, K., Yoshida, N., Kishimoto, T., and Akira, S. (1996) *Nature* **380**, 627–630
41. Nakayama, T., June, C. H., Munitz, T. I., Sheard, M., McCarthy, S. A., Sharrow, S. O., Samelson, L. E., and Singer, A. (1990) *Science* **249**, 1558–1561
42. Omori, M., Yamashita, M., Inami, M., Ukai-Tadenuma, M., Kimura, M., Nigo, Y., Hosokawa, H., Hasegawa, A., Taniguchi, M., and Nakayama, T. (2003) *Immunity* **19**, 281–294
43. Ward, S. G., Wilson, A., Turner, L., Westwick, J., and Sansom, D. M. (1995) *Eur. J. Immunol.* **25**, 526–532
44. Traenckner, E. B., Pahl, H. L., Henkel, T., Schmidt, K. N., Wilk, S., and Baeuerle, P. A. (1995) *EMBO J.* **14**, 2876–2883
45. Zhou, M., Gu, L., Zhu, N., Woods, W. G., and Findley, H. W. (2003) *Oncogene* **22**, 8137–8144
46. Sun, S. C., Ganchi, P. A., Ballard, D. W., and Greene, W. C. (1993) *Science* **259**, 1912–1915
47. Asnagli, H., Afkarian, M., and Murphy, K. M. (2002) *J. Immunol.* **168**, 4268–4271
48. Kishikawa, H., Sun, J., Choi, A., Miaw, S. C., and Ho, I. C. (2001) *J. Immunol.* **167**, 4414–4420
49. Lavenu-Bombled, C., Trainor, C. D., Makeh, I., Romeo, P. H., and Max-Audit, I. (2002) *J. Biol. Chem.* **277**, 18313–18321
50. Perkins, N. D., Felzien, L. K., Betts, J. C., Leung, K., Beach, D. H., and Nabel, G. J. (1997) *Science* **275**, 523–527
51. Sheppard, K. A., Rose, D. W., Haque, Z. K., Kurokawa, R., McInerney, E., Westin, S., Thanos, D., Rosenfeld, M. G., Glass, C. K., and Collins, T. (1999) *Mol. Cell. Biol.* **19**, 6367–6378
52. Zhong, H., May, M. J., Jimi, E., and Ghosh, S. (2002) *Mol. Cell* **9**, 625–636
53. Holloway, A. F., Rao, S., Chen, X., and Shannon, M. F. (2003) *J. Exp. Med.* **197**, 413–423
54. Ghosh, S., and Karin, M. (2002) *Cell* **109**, (suppl.) 81–96
55. Li, Q., and Verma, I. M. (2002) *Nat. Rev. Immunol.* **2**, 725–734
56. Johnson, K., Angelin-Duclos, C., Park, S., and Calame, K. L. (2003) *Mol. Cell. Biol.* **23**, 2438–2450
57. Kouzarides, T. (2002) *Curr. Opin. Genet. Dev.* **12**, 198–209

THE JOURNAL OF BIOLOGICAL CHEMISTRY
Vol. 279, No. 26, Issue of June 25, pp. 26983–26990, 2004
Printed in U.S.A.

Essential Role of GATA3 for the Maintenance of Type 2 Helper T (Th2) Cytokine Production and Chromatin Remodeling at the Th2 Cytokine Gene Loci*

Received for publication, April 2, 2004
Published, JBC Papers in Press, April 15, 2004, DOI 10.1074/jbc.M403688200

Masakatsu Yamashita‡§¶, Maki Ukai-Tadenuma‡¶, Takeshi Miyamoto§, Kaoru Sugaya‡§, Hiroyuki Hosokawa§, Akihiro Hasegawa§, Motoko Kimura§, Masaru Taniguchi‖, James DeGregori‡‡, and Toshinori Nakayama§ §§**

*From the ‡PRESTO Project, Japan Science and Technology Corporation (JST), §Department of Immunology, Graduate School of Medicine, Chiba University, 1-8-1 Inohana Chuo-ku, Chiba 260-8670, Japan, the ‖Laboratory for Immune Regulation, RIKEN Research Center for Allergy and Immunology, Yokohama 230-0045, Japan, and the **Department of Biochemistry and Molecular Genetics, University of Colorado Health Sciences Center, BRB802, Denver, Colorado 80262*

GATA3 expression is essential for type-2 helper T (Th2) cell differentiation. GATA3-mediated chromatin remodeling at the Th2 cytokine gene loci, including Th2-specific long range histone hyperacetylation of the interleukin (IL)-13/IL-4 gene loci, occurs in developing Th2 cells. However, little is known about the role of GATA3, if any, in the maintenance of established remodeled chromatin at the Th2 cytokine gene loci. Here, we established a Cre/LoxP-based site-specific recombination system in cultured CD4 T cells using a unique adenovirus-mediated gene transfer technique. This system allowed us to investigate the effect of loss of GATA3 expression in *in vitro* differentiated Th2 cells. After ablation of GATA3, we detected reduced production of all Th2 cytokines, increased DNA methylation at the IL-4 gene locus, and decreased histone hyperacetylation at the IL-5 gene locus but not significantly so at the IL-13/IL-4 gene loci. Thus, GATA3 plays important roles in the maintenance of the Th2 phenotype and continuous chromatin remodeling of the specific Th2 cytokine gene locus through cell division.

After antigenic stimulation, naive CD4 T cells differentiate into two distinct helper T cell (Th)[1] subsets, Th1 and Th2 cells (1). Th1 cells produce IFN-γ to control cell-mediated immunity against intracellular pathogens. Th2 cells produce IL-4, IL-5, and IL-13, and are involved in humoral immunity and allergic reactions (2–4). The outcome of Th cell differentiation depends on the cytokine environment (5, 6). IL-4-mediated STAT6 activation is important for inducing efficient Th2 cell generation (7, 8), although IL-4/STAT6-independent Th2 responses have also been reported in various experimental systems (9–13).

Recent studies have identified several transcription factors that control Th2 cell differentiation (8, 14, 15). Among them, GATA3 appears to be a master transcription factor for Th2 cell differentiation. GATA3 is selectively expressed in Th2 cells and its ectopic expression induces Th2 cell differentiation even in the absence of STAT6 (16–19). Also, GATA3-dependent autoactivation (13, 19) and an instructive role of GATA3 for Th2 cell differentiation (20) were reported.

Changes in the chromatin structure of the Th2 cytokine (IL-4/IL-5/IL-13) gene loci occur during Th2 cell differentiation (14, 21). Th2 cell differentiation induced by ectopic expression of GATA3 results in DNA demethylation (21) and the induction of DNase I-hypersensitive sites in the IL-4 gene locus (19, 22). Recently, we and others demonstrated that histone hyperacetylation of the Th2 cytokine gene loci occurs in developing Th2 cells in a Th2-specific and STAT6-dependent manner (23–25). We demonstrated an essential role for GATA3 in Th2-specific histone hyperacetylation (23). We generated a precise map of the Th2-specific histone hyperacetylation within the type 2 cytokine gene loci, and identified a 71-bp conserved GATA3 response element (CGRE) 1.6 kbp upstream of the IL-13 locus exon 1 (23). The conserved GATA3 response element (CGRE) may play a crucial role for GATA3-mediated targeting and downstream spreading of core histone hyperacetylation within the IL-13 and IL-4 gene loci in developing Th2 cells. However, it is still unclear whether continuous expression of GATA3 is required for the maintenance of the established chromatin remodeling at the Th2 cytokine gene loci.

In the present study, we investigated the role for GATA3 in the maintenance of Th2 cytokine production and the remodeled chromatin using a newly established *in vitro* site-specific recombination system. The loss of GATA3 expression resulted in decreased Th2 cytokine production, reduction of histone hyperacetylation at the IL-5 gene locus, and increased DNA methylation at the IL-4 gene locus. Thus, GATA3 plays important roles in the maintenance of the Th2 phenotype and continuous chromatin remodeling of the specific Th2 cytokine gene loci.

* This work was supported by Ministry of Education, Culture, Sports, Science and Technology (Japan) Grants-in-Aid for Scientific Research, Priority Areas Research 13218016, 12051203, Scientific Research B 14370107, and Special Coordination Funds for Promoting Science and Technology, the Ministry of Health, Labor and Welfare (Japan), the Program for Promotion of Fundamental Studies in Health Science of the Organization for Pharmaceutical Safety and Research (Japan), Uehara Memorial Foundation, Hamaguchi Foundation, and Kanae Foundation. The costs of publication of this article were defrayed in part by the payment of page charges. This article must therefore be hereby marked "*advertisement*" in accordance with 18 U.S.C. Section 1734 solely to indicate this fact.

¶ Both authors contributed equally to this study.

‡‡ Supported by a Scholar award from the Leukemia and Lymphoma Society and National Institutes of Health NCI Grant RO1 CA77314.

§§ To whom correspondence should be addressed: Dept. of Immunology, Graduate School of Medicine, Chiba University, 1-8-1 Inohana, Chuo-ku, Chiba 260-8670 Japan. Tel.: 81-43-226-2200; Fax: 81-43-227-1498; E-mail: tnakayama@faculty.chiba-u.jp.

[1] The abbreviations used are: Th, helper T; TCR, T cell antigen receptor; STAT, signal transducer and activator of transcription; CAR, coxsackie/adenovirus receptor; EGFP, enhanced green fluorescence protein; ChIP, chromatin immunoprecipitation; STAT6-KO, signal transducer and activator of transcription 6-deficient; IL, interleukin; mAb, monoclonal antibody; GFP, green fluorescent protein; ELISA, enzyme-linked immunosorbent assay; Ad, adenovirus; IFU, infection units; PE, phycoerythrin.

EXPERIMENTAL PROCEDURES

Mice—C57BL/6 mice were purchased from SLC (Shizuoka, Japan). STAT6-deficient mice were kindly provided by Dr. Shizuo Akira (Osaka University, Japan) (26). Transgenic mice expressing coxsackie/adenovirus receptor under the control of an *lck* proximal promoter (coxsackie/adenovirus receptor (CAR) Tg mice) has been previously described (27). All mice used in this study were maintained under specific pathogen-free conditions and were used at 4–6 weeks of age. Animal care was in accordance with the guidelines of Chiba University.

Immunofluorescent Staining and Flow Cytometry Analysis—In general, one million cells were stained with antibodies as indicated according to a standard method (28). Anti-CD4-fluorescein isothiocyanate (RM4-1-FITC) and anti-CD8-PE (53.6-72-PE) were purchased from BD Pharmingen. For detecting hCAR, biotinylated anti-CAR antibody (RmcB) (27) and Cy5-conjugated avidin were used. For intracellular staining, allophycocyanin-conjugated anti-IFN-γ antibody (XMG1.2; BD Pharmingen), anti-IL-5 antibody (TRFK5; BD Pharmingen), and PE-conjugated anti-IL-4 antibody (11B11; BD Pharmingen) were used (29, 30). Flow cytometry analysis was performed on FACScalibur (BD Biosciences) and results were analyzed with CELLQUEST software (BD Biosciences).

In Vitro T Cell Differentiation Culture—Purification and *in vitro* Th cell differentiation cultures were done as described (23, 29). Splenic CD4 cells were purified using magnetic beads and an Auto-MACS Sorter™ (Miltenyi Biotec), yielding purity of >98%. For Th1 differentiation, the cells (1.5×10^6) were stimulated for 2 days with immobilized anti-TCR mAb (H57-597; BD Pharmingen) and anti-CD28 mAb (37.51; BD Pharmingen) in the presence of IL-2 (25 units/ml), IL-12 (100 units/ml), and anti-IL-4 mAb (11B11, 25% culture supernatant). For Th2 cell differentiation, cells were stimulated with immobilized anti-TCR mAb and anti-CD28 mAb for 2 days in the presence of IL-2 (25 units/ml), IL-4 (100 units/ml), and anti-IFNγ mAb (R4-6A2, 25% culture supernatant). The cells were then transferred to new wells and cultured for another 3 days in the presence of only the cytokines present in the initial culture. In some experiments, two or three cycles of the anti-TCR plus anti-CD28 stimulation were used.

Virus Vectors, Infection, and Strategy for Deletion of GATA3 Transgene—The retroviral vector pMX-IRES-EGFP and a Plat-E packaging cell line were kindly provided by Dr. Toshio Kitamura (University of Tokyo, Tokyo, Japan). Retrovirus vectors containing a *loxP*-flanked EGFP cassette (pMX-loxP-EGFP-loxP) and a *loxP*-flanked human GATA3-IRES-EGFP cassette (pMX-loxP-GATA3-IRES-EGFP-loxP) were generated using the original pMX-IRES-GFP vector (31) (Fig. 1*A*). The method for the preparation of virus supernatant was described previously (32). An adenovirus vector containing a Cre recombinase expression cassette (Ad-Cre) was kindly provided by Izumi Saito (University of Tokyo, Tokyo, Japan) (Fig. 1*B*) (33).

To investigate the effect of loss of GATA3 expression in differentiated Th2 cells, we established a site-specific recombination system in CD4 T cells cultured *in vitro*. The strategy of introduction and deletion of the GATA3 transgene is illustrated in Fig. 1*C*. First, naive CD4 T cells were stimulated under Th1-skewed conditions, and infected with retrovirus vectors containing a *loxP*-flanked GATA3/IRES/EGFP cassette. Three days later, GFP-positive retrovirus-infected cells were sorted with a FACSVantage (BD Biosciences) flow cytometer and restimulated under the same Th1-skewed conditions of initial stimulation for a further 5 days. After another cycle of 5-day re-stimulation culture under Th1-skewed conditions, the cells were infected with Ad-Cre to delete the GATA3/IRES/EGFP transgene by expressing NLS-tagged Cre recombinase. The preparation of adenovirus supernatant was done as described (33). Cell entry by adenovirus involves high-affinity binding of the viral fiber capsid protein to a cellular receptor, CAR. We used CAR Tg mouse T cells to avoid the limited expression of CAR on T cells (27).

In Figs. 4 and 5, a more strict protocol was used. The outline of the protocol is shown in Fig. 4*A*. Four days after infection of retrovirus vectors containing a *loxP*-flanked GATA3/IRES/EGFP, cells were stimulated with immobilized anti-TCR and anti-CD28 for 4 h, stained with anti-IL-4 PE detection mAbs using IL-4 Secretion Assay kit (number 130-090-515; Militenyi Biotec), and $GFP^+IL\text{-}4^+$ cells were sorted with purity >98%. The sorted cells were cultured for 6 days in the presence of cytokines (IL-2 and IL-12), and then another stimulation with anti-TCR and anti-CD28 was performed. Two days later, cells were infected with Ad-Cre. Four days after Ad-Cre infection, GFP^- cells were sorted to exclude the small numbers of GFP^+ (GATA3) expressing cells remaining in the culture. After T cell expansion by anti-TCR stimulation, analysis was done on day 25. To exclude the effect of endogenously induced GATA3 molecules, we used naive STAT6-deficient CD4 T cells and Th1-skewed culture conditions containing anti-IL-4 mAb throughout the 25-day cultivation.

PCR Analysis—The levels of EGFP transgene were assessed by semi-quantitative PCR with a specific primer pairs: forward, GTGAACCGTCAGATCCG-3′ and reverse, 5′-TTACTTGTACAGCTCGTC.

Immunoblot Analysis—The amounts of GATA3 and GFP were assessed by immunoblotting with anti-GATA3 mouse mAb, HG3-31 (Santa Cruz Biotechnology, Santa Cruz, CA), and anti-GFP antiserum (MBL, Nagoya, Japan) as described (30).

ELISA for the Measurement of Cytokine Concentration—Cells were stimulated with immobilized anti-TCR (3 μg/ml) in 48-well flat bottom plates (2.5×10^5 cells/well) for 24 h at 37 °C. The production of IL-4, IL-5, IFN-γ, and IL-2 was assessed by ELISA as described previously (30). The production of IL-13 was evaluated with a mouse IL-13 ELISA kit (R & D Systems) according to the manufacturer's protocol.

Reverse Transcriptase-PCR—Total RNA was isolated from cultured cells using the TRIzol reagent. Reverse transcription was carried out with Superscript II RT (Invitrogen). Three-fold serial dilutions of template cDNA were done. The primers used were as described previously (32).

Chromatin Immunoprecipitation (ChIP) Assay—ChIP assays were performed using histone H3 ChIP assay kits (number 17-245; Upstate Biotechnology) and specific primers as described previously (23).

Methylation-specific PCR—Genomic DNA was isolated from 1×10^6 cells by using a Wizard Genomic DNA Purification kit (Promega). Bisulfate treatment of DNA was performed by using a CpGenome DNA Modification kit (Intergen, Purchase, NY). The sequences of primers used for PCR amplification were described previously by Guo *et al.* (34).

RESULTS

Efficient Adenovirus-mediated Transgene Introduction into CAR Tg CD4 T Cells in Vitro—The aim of this study was to determine the role of GATA3, if any, in the maintenance of the established Th2 phenotype and Th2-type chromatin remodeling. To investigate the effect of loss of GATA3 expression in differentiated Th2 cells, we established a Cre/loxP-mediated site-specific recombination system in T cells. The system constitutes (i) retrovirus-mediated introduction of a *loxP*-flanked GATA3 transgene for Th2 cell differentiation from naive CD4 T cells, and (ii) subsequent adenovirus-mediated Cre expression to delete the *loxP*-flanked GATA3 transgene (Fig. 1).

Thus, we first evaluated the feasibility of adenovirus-mediated gene transfer in T cells. Naive CD4 T cells express limited amounts of CAR and are known to be resistant to adenovirus infection. To increase the efficiency of adenovirus infection in T cells, we used CAR Tg mice expressing CAR on T cells under the control of the proximal promoter of *lck* and a CD2 enhancer, in which the majority of CD4 and CD8 T cells in the spleen showed high level cell surface expression of CAR (27). Freshly prepared CD4 T cells from CAR Tg mice were infected with Ad-EGFP. Two days after infection, the majority of CAR Tg CD4 T cells expressed substantial levels of GFP compared with that of non-Tg B6 CD4 T cells (Fig. 2*A*). A time course of the GFP expression after Ad-EGFP infection was assessed in CAR CD4 T cells cultured under Th1- or Th2-skewed conditions (Fig. 2*B*). The expression of GFP peaked on day 3 in either Th1 or Th2-skewed culture conditions. The high-level expression was maintained for at least 4 days after infection. Thus, adenovirus-mediated gene transfer was efficient when using CD4 T cells from CAR Tg mice.

Deletion of a loxP-flanked EGFP Transgene by Ad-Cre Infection in Cultured CD4 T Cells—The efficiency of Cre-mediated DNA recombination was next assessed in CAR Tg CD4 T cells using EGFP as an indicator. CAR Tg CD4 T cells were stimulated with anti-TCR mAb plus anti-CD28 mAb and infected with a retrovirus containing a *loxP*-flanked EGFP cassette (pMX-loxP-EGFP-loxP). GFP-expressing infected cells were sorted, restimulated for 3 days, and then infected with either 1 or 3×10^8 IFU of Ad-Cre as described under "Experimental Procedures." Fig. 3*A* shows a representative genomic DNA PCR result assessing the amount of EGFP transgene DNA left in

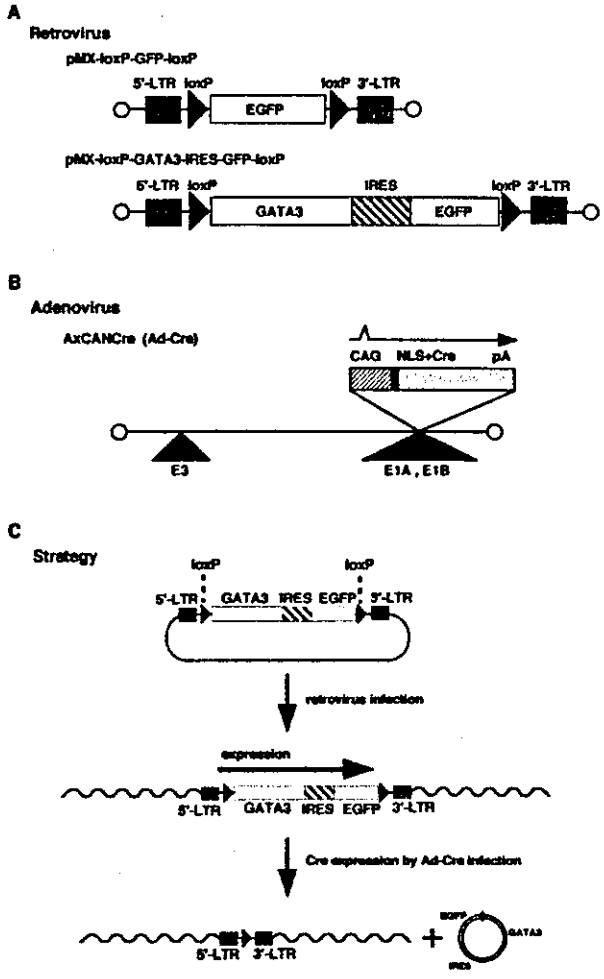

FIG. 1. **Schematic representation of retrovirus and adenovirus vectors, and strategy for Cre-mediated site-specific gene recombination.** *A*, retrovirus vectors containing *loxP*-flanked EGFP (pMX-loxP-EGFP-loxP) and *loxP*-flanked human GATA3-IRES-EGFP (pMX-loxP-GATA3-IRES-EGFP-loxP). *B*, an adenovirus vector inserted with the Cre recombinase gene (*Ad-Cre*). *C*, the strategy for introduction and deletion of the GATA3 transgene.

CD4 T cells after Ad-Cre infection. The ratio of EGFP/input DNA is shown in Fig. 3*B*. The EGFP transgene content was significantly decreased 2 days after Ad-Cre infection in a virus-dosage dependent manner. On day 3, the majority of the EGFP transgene was deleted by infection with 3×10^8 IFU of Ad-Cre (Fig. 3*A*, *bottom*). These results suggest that the *lox-P*-flanked EGFP transgene was efficiently deleted in cultured CD4 T cells by Ad-Cre infection when CAR Tg CD4 T cells are used.

Concurrently, the expression levels of EGFP protein after Ad-Cre infection were monitored by flow cytometry. To allow comparison with the EGFP-negative T cell control peak, no GFP sorting was done in this particular experiment. Shown are representative flow cytometry histograms (Fig. 3*C*), and relative intensity data from the GFP-positive peaks after infection with 3×10^8 IFU of Ad-Cre (Fig. 3*D*). As can be seen, expression levels of GFP in CAR Tg CD4 T cells decreased day by day after Ad-Cre infection, and were approximately one-fifth of the original expression level on day 4 when 3×10^8 IFU of Ad-Cre were used (Fig. 3*D*). In contrast, only a marginal decrease was observed in non-Tg CD4 T cell cultures. Although almost complete deletion of the EGFP transgene was detected on day 3 post-infection with 3×10^8 IFU of Ad-Cre (see Fig. 3, *A* and *B*), a significant amount of GFP protein (~20–30%) was detected by flow cytometry. This could be explained by the substantially long half-life of the GFP protein.

Efficient Depletion of Retrovirus-induced GATA3 Expression by Ad-Cre Infection in in Vitro Differentiated Th2 Cells—To investigate the role of GATA3 in the maintenance of the Th2 phenotype, CD4 T cells from STAT6-deficient CAR Tg mice cultured under Th1-skewed conditions were infected with retroviral vectors containing a *lox-P*-flanked GATA3/IRES/GFP cassette (pMx-loxP-GATA3-IRES-GFP-loxP). In the STAT6-deficient T cells cultured under Th1-skewed conditions, endogenous GATA3 induction was minimum. The outline of the protocol is shown in Fig. 4*A*. Four days after infection of the retrovirus vector, the cells were stimulated with immobilized anti-TCR and anti-CD28 mAb, stained with anti-IL-4-PE detection mAbs, and $GFP^+IL\text{-}4^+$ cells were sorted. Representative GFP/IL-4 profiles are shown in Fig. 4*B*. The sorted cells were cultured for 6 days in the presence of cytokines (IL-2 and IL-12), and another cycle of stimulation with anti-TCR and anti-CD28 was performed on day 12. Two days later, the cells were infected with Ad-Cre (3×10^8 IFU). Four days after Ad-Cre infection, GFP^- cells were sorted to enrich for GATA3 transgene-depleted cells. Th1-skewed conditions were used throughout the 25-day culture. The cultured cells were harvested, and the expression levels of EGFP and GATA3 were assessed to confirm that GATA3 protein is depleted (Fig. 4, *C* and *D*). As can be seen, the levels of GFP fluorescence were reduced (Fig. 4*C*), and the expression levels of GATA3 protein were decreased dramatically (about 10-fold) in the cells infected with Ad-Cre (Fig. 4*D*). Without Ad-Cre infection, the expression of GATA3 protein was not changed during the last 7-day cultivation (data not shown).

The mRNA levels of several transcriptional regulators (GATA3, c-Maf, JunB, and T-bet) in the Th2 cells after ablation of GATA3 were assessed (Fig. 4*E*). As expected, the mRNA levels of GATA3 were ~1/10 of those of LacZ-infected control cells. In contrast, essentially no significant change in c-Maf or JunB expression was detected in the Ad-Cre-infected T cells. The expression of T-bet was reduced by the expression of GATA3, and restored by the depletion of GATA3 transgene.

Expression of GATA3 Is Required for Th2 Cytokine Production in in Vitro Differentiated Th2 Cells—Cytokine production profiles of the cells prepared in Fig. 4 were assessed by cytoplasmic staining. As can be seen in Fig. 5*A*, *middle panels*, more than 40% (39.3 + 3.5%) of the cells infected with pMx-loxP-GATA3-IRES-GFP-loxP were IL-4 producing cells, and more than 30% (19.2 + 18.2%) were IL-5 producing cells. Marginal numbers of IFN-γ producing IL-4 non-producing cells were detected (7.0%). The percentages of IL-4 producing cells were decreased to about 25% (23.1 + 3.8%) after Ad-Cre infection, and those of IL-5 were about 16% (8.1 + 7.9%) (compare the percentages depicted in the *middle* and *right panels* in IFN-γ/IL-4 and IL-5/IL-4 profiles). A significant number of IFN-γ producing cells was noted, suggesting that some of the cells become IFN-γ producing cells after depletion of the GATA3 transgene. These results suggest that GATA3 expression is important for the maintenance of Th2 cytokine production.

Next, the levels of Th2 cytokines produced in the culture supernatant were determined by ELISA. Little in the way of Th2 cytokines (IL-4, IL-13, and IL-5) were detected in supernatants from non-infected cells cultured under Th1-skewed conditions. In contrast, GATA3-transduced cells produced large amounts of Th2 cytokines and decreased amounts of Th1 cytokines (IFN-γ and IL-2) as previously reported (16–19). As

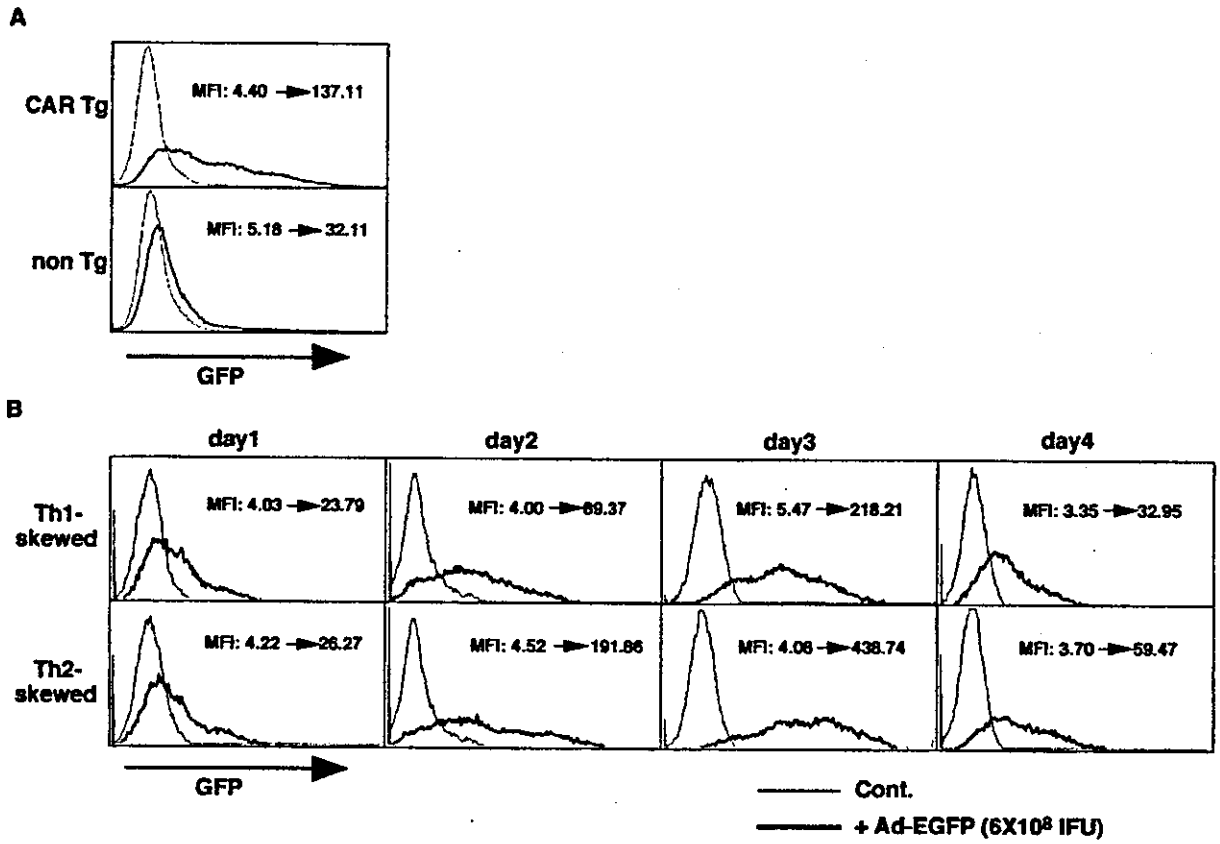

FIG. 2. **Efficient transgene introduction into CAR Tg CD4 T cells using adenovirus vector.** The EGFP gene was cloned into the adenovirus vector (*Ad-EGFP*). Freshly prepared CAR Tg and normal non-Tg CD4 T cells (*A*) and cultured CAR CD4 T cells under Th1- and Th2-skewed conditions were infected with Ad-EGFP. Assays were done on day 2 (*A*) or on the indicated day (*B*) after Ad-EGFP infection. The efficiency of Ad-EGFP transgene expression was assessed in flow cytometry using GFP fluorescence as an indicator. Mean fluorescence intensity (*MFI*) is depicted in each panel.

expected, the production of Th2 cytokines (IL-4, IL-13, and IL-5) was significantly decreased by Ad-Cre infection (Fig. 5*B*, *bottom*). IFN-γ production was moderately restored. These results suggest that the continuous expression of GATA3 is important for the production of IL-4, IL-5, and IL-13 in the *in vitro* differentiated Th2 cells.

GATA3 Is Required for the Maintenance of Hyperacetylation of Histone H3 in the IL-5 Gene Locus but Not in the IL-13/IL-4 Gene Loci—Finally, we assessed the chromatin remodeling status of the Th2 cytokine gene loci after deletion of the GATA3 transgene. Acetylation status of histone H3 (K9/14) in the nucleosomes associated with the Th2 cytokine gene loci was determined by ChIP assays. The levels of acetylation in *in vitro* differentiated Th2 cells cultured under Th2-skewed conditions for 5 days are shown for comparison. The relative band intensities (Ac-H3/Input DNA) are shown in Fig. 6*B*. As we reported previously, ectopic expression of GATA3 induced histone hyperacetylation in the Th2 cytokine gene loci (Fig. 6*A*, *Ac-H3*, *second column*) (23). As shown in Fig. 6, *A* and *B*, significantly reduced histone hyperacetylation of the IL-5 promoter region was detected by the Ad-Cre-mediated deletion of the GATA3 transgene. The decrease in the acetylation of IL-4 promoter, IL-13 promoter, V_A enhancer, CNS1, and GATA3 response element was marginal. Acetylation of the IFNγ promoter was decreased by GATA3 expression, and significantly increased by deletion of the GATA3 transgene (Fig. 6, *A* and *B*, *bottom*).

GATA3 Is Required for the Maintenance of Continuous Demethylation of the IL-4 Intron 2 Region—Demethylation of the IL-4 intron 2 region in developing Th2 and established Th2 cells was reported previously (21). Here, we used a methylation-specific PCR technique to evaluate the methylation status of IL-4 intron 2 (34). After treatment of genomic DNA with bisulfate, unmethylated cytidine is converted to uridine but methylcytidine is preserved as cytidine. In this system, primers that distinguish uridine (thymidine) and cytidine at sites of CpGs were used to evaluate the levels of methylation. We focused on two cytidine residues within the IL-4 intron 2 region, and four patterns (both methylated, M/M; one methylated and one demethylated, M/U or U/M; and both demethylated, U/U) would be detected. In GATA3 non-transduced cells, 50% of the genome contained methylated cytidine at both residues (Fig. 6, *C* and *D*, *top*). In GATA3-transduced cells, only 20% of this region was methylated at both residues, 40% was unmethylated and 40% was hemimethylated (Fig. 6, *C* and *D*, *middle*). When the GATA3 transgene was deleted, 50% of the genome contained both cytidine residues methylated, and only 20% was unmethylated (Fig. 6, *C* and *D*, *bottom*), suggesting that the methylation pattern was compatible to that of non-GATA3 transduced cells. These results suggest that continuous GATA3 expression is required to maintain the unmethylated status of the Th2 cytokine gene loci in differentiated Th2 cells.

DISCUSSION

In the present study, we established a Cre/LoxP-based site-specific recombination system in cultured CD4 T cells using a unique adenovirus-mediated gene transfer technique. Ectopic

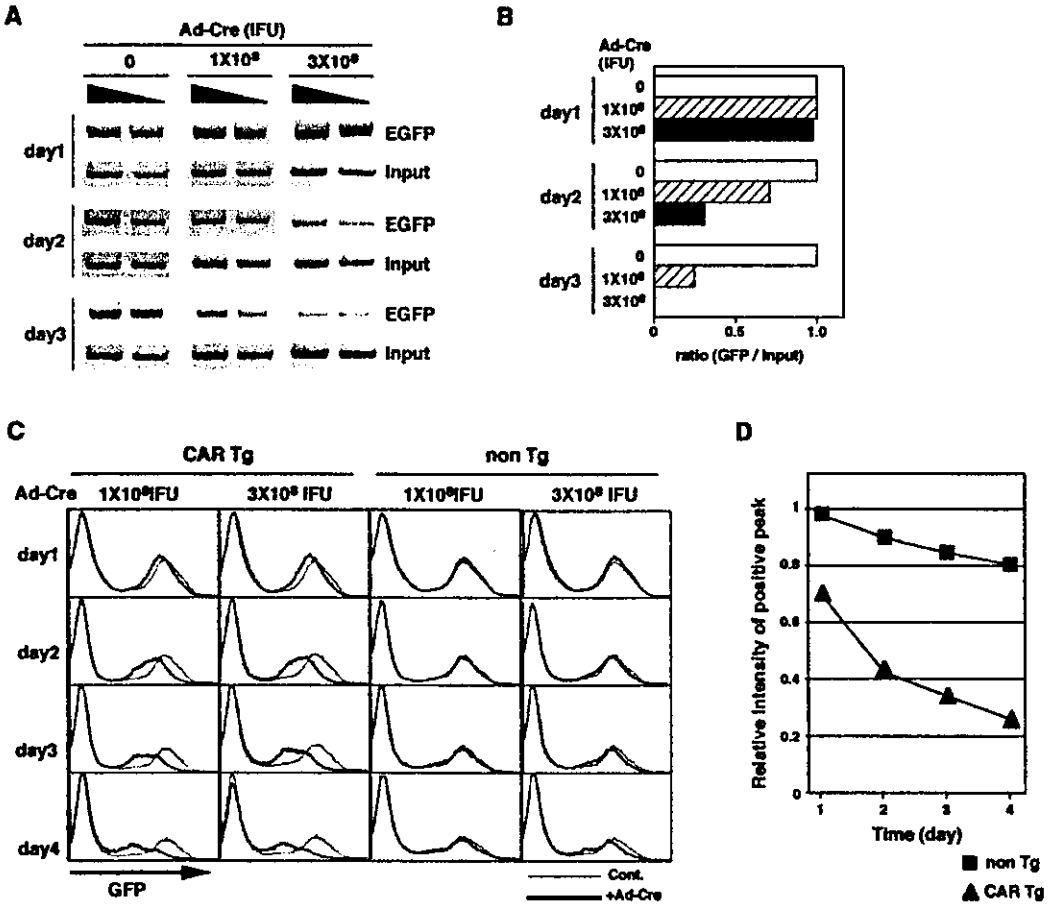

FIG. 3. **Deletion of a *loxP*-flanked EGFP transgene by Ad-Cre infection in cultured CD4 T cells.** CAR Tg CD4 T cells were stimulated with anti-TCR mAb plus anti-CD28 mAb and infected with a retrovirus containing *loxP*-flanked EGFP (pMX-loxP-EGFP-loxP). GFP expressing infected cells were sorted, restimulated for 3 days, and then infected with 1×10^8 or 3×10^8 IFU of Ad-Cre. *A*, a representative genomic semi-quantitative PCR of the EGFP transgene. *B*, the ratios of EGFP/input DNA. *C*, CAR Tg and non-Tg CD4 T cells were stimulated with anti-TCR mAb plus anti-CD28 mAb, and infected with a retrovirus containing *loxP*-flanked EGFP (pMX-loxP-EGFP-loxP). The expression levels of GFP protein in whole cells (both retrovirus-infected and uninfected populations) were monitored by flow cytometry after 1×10^8 and 3×10^8 IFU Ad-Cre infection. The relative intensity of the positive peak of 3×10^8 IFU Ad-Cre infection is depicted in *panel D*.

expression of GATA3 induced Th2 cell generation without IL-4 or STAT6 activation. Using these Th2 cells, the role of GATA3 expression in the maintenance of Th2 phenotype was examined by deleting the GATA3 transgene with adenovirus-mediated expression of the Cre protein. The reduction of GATA3 expression in the *in vitro* differentiated Th2 cells resulted in decreased production of all Th2 cytokines tested (IL-4, IL-13, and IL-5) (Fig. 5), decreased histone hyperacetylation of the IL-5 gene locus (Fig. 6, *A* and *B*), and increased methylation of DNA at the IL-4 intron 2 region (Fig. 6, *C* and *D*). These results suggest that continuous expression of GATA3 is required for the maintenance of Th2 cytokine production and remodeled open chromatin at the specific Th2 cytokine gene loci.

The production of Th2 cytokines, particularly IL-5 and IL-13, were reported to be highly dependent on the transcriptional activity of GATA3 (16, 35, 36). We reported that expression of GATA3 induced more than a 10-fold increase in IL-5 and IL-13 promoter activities, whereas that of the IL-4 promoter was increased only about 2-fold (23). Therefore, the decreased IL-5 and IL-13 production after deletion of the GATA3 transgene by Cre-induced recombination is explained at least in part by the decreased transcriptional activity of GATA3.

More importantly, however, we detected decreased histone hyperacetylation at the IL-5 gene locus and increased methylation of IL-4 gene intron 2 following GATA3 ablation (Fig. 6), suggesting that the levels of openness of chromatin at specific Th2 cytokine gene loci were dependent on the expression of GATA3. Interestingly, the levels of acetylation at the IL-13/IL-4 gene loci were not significantly affected by the ablation of the GATA3 protein (Fig. 6). It is possible that small amounts of residual GATA3 are sufficient for the maintenance of acetylation of the IL-13/IL-4 gene loci but not for that of the IL-5 locus. Alternatively, GATA3 independent molecular events that maintain the histone hyperacetylation are operating at the IL-13/IL-4 gene loci in differentiated Th2 cells. Histone H3-K4 methylation and histone H3-K9/14 acetylation appear to be associated with transcriptionally active chromatin (37). Disruption of an H3-K4-specific methyltransferase, MLL containing a SET domain, resulted in reduced histone acetylation (38, 39). Thus, unknown but critical molecular events may control histone H3-K9/14 acetylation as well as histone H3-K4 methylation in *in vitro* differentiated Th2 cells.

Recently, we have reported that the induction of histone hyperacetylation at the IL-5 gene locus is dependent on STAT6 and GATA3, but the signal requirements are distinct from that for the IL-13/IL-4 gene loci (40). The remodeling process of the IL-5 gene locus is more sensitive to CD28-induced NF-κB activation. It is possible that molecular events governing the maintenance of histone hyperacetylation of the IL-13/IL-4 gene loci and that of IL-5 locus are distinct.

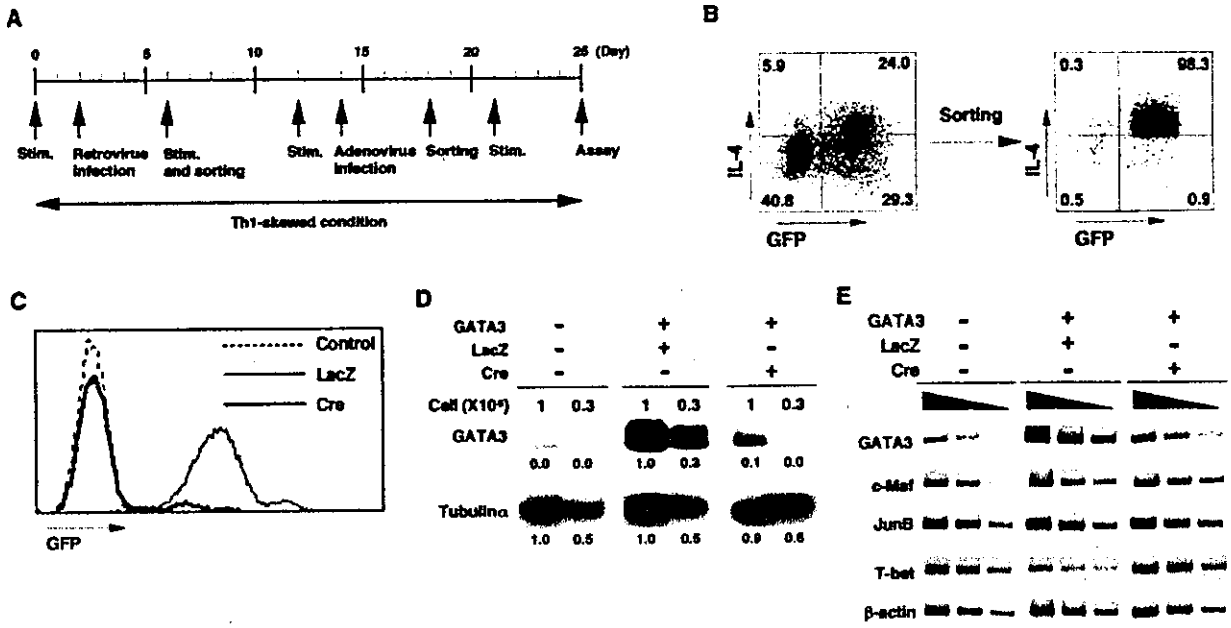

FIG. 4. **Depletion of retrovirus-induced GATA3 expression by Ad-Cre infection in *in vitro* differentiated Th2 cells.** *A*, the outline of the protocol for GATA3-depletion in Th2 cells. Naive CD4 T cells from CAR Tg mice with a STAT6-deficient background were stimulated (*stim.*) under Th1-skewed conditions, and infected with retrovirus vectors containing a *loxP*-flanked GATA3/IRES/EGFP cassette on day 2. Four days after infection with retrovirus vectors, the cells were stimulated with immobilized anti-TCR and anti-CD28 for 4 h, stained with anti-IL-4 PE detection mAbs, and $GFP^+IL\text{-}4^+$ cells were sorted. The sorted cells were cultured for 6 days in the presence of cytokines (IL-2 and IL-12), and another stimulation with anti-TCR and anti-CD28 was performed. Two days later, the cells were infected with either Ad-Cre (3×10^8 IFU) or Ad-LacZ (3×10^8 IFU). Four days after adenovirus infection, GFP^- cells were sorted to enrich the GATA3 transgene-depleted cells. After T cell expansion by anti-TCR/anti-CD28 stimulation, analysis was done on day 25. *B*, representative GFP/IL-4 profiles on sorted cells at day 6. Cells were stained with anti-IL-4 PE as described in *A* and GFP/IL-4 double positive cells were sorted by flow cytometry. The percentages of cells in each quadrant are shown. *C*, expression levels of EGFP in the *in vitro* differentiated Th2 cells with or without Ad-Cre infection. An Ad-LacZ vector was used as a control. The expression level of EGFP in the cells (on day 25) prepared as in *panel A* was determined by flow cytometry. *D*, immunoblot analysis for GATA3 in the *in vitro* differentiated Th2 cells with or without Ad-Cre infection. GATA3 and tubulin α expression levels were determined by immunoblotting with specific mAbs. Lysates from 3×10^6 (*upper* for GATA3) and 0.3×10^6 (*lower* for tubulin α) cells were used per lane. The results are representative of three independent experiments. Arbitrary densitometric units are depicted under each band. *E*, expression levels of Th2- and Th1-related transcriptional regulators in Th2 cells depleted of the GATA3 transgene. The transcription levels of GATA3, c-Maf, JunB, T-bet, and β-actin were determined by semiquantitative reverse transcriptase-PCR analysis with 3-fold serial dilution of template cDNA.

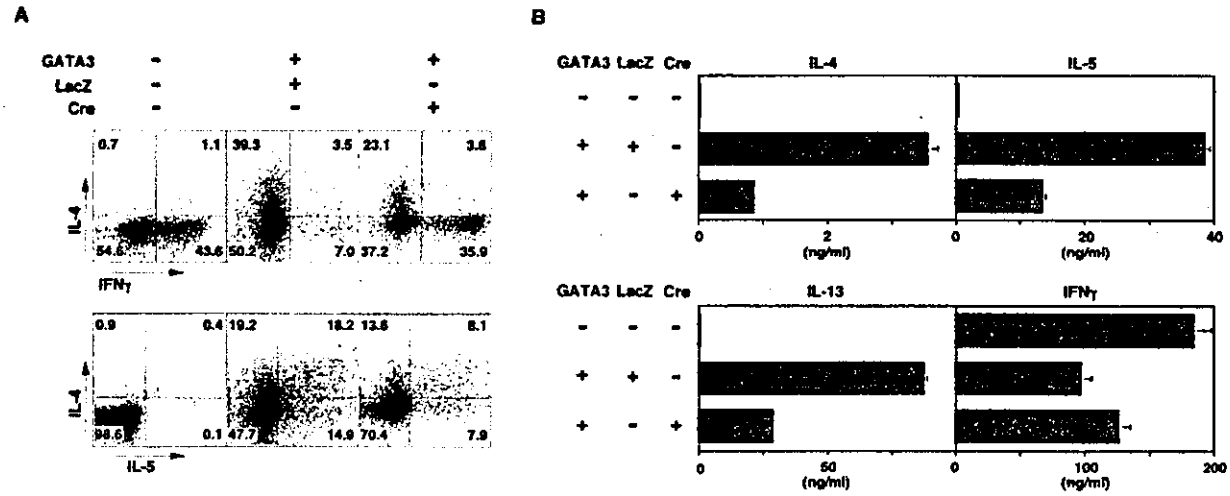

FIG. 5. **Effect of GATA3 depletion on Th2 cytokine production in *in vitro* differentiated Th2 cells.** *A*, cytokine production profiles of Th2 cells after depletion of the GATA3 transgene prepared as in Fig. 4*A* were assessed by cytoplasmic staining (IFN-γ/IL-4 and IL-5/IL-4). The percentages of the cells present in each quadrant are shown. Four independent experiments were done with similar results. *B*, cytokine production of Th2 cells after depletion of the GATA3 transgene was assessed by ELISA. Four independent experiments were done with similar results.

We also demonstrated that GATA3 expression is required for the maintenance of demethylation of the IL-4 intron 2 region (Fig. 6, *C* and *D*). It is not clear whether GATA3 is involved directly in the methylation processes of the methyltransferase complex at this time. Recently, Tamaru *et al.* (42) reported that methylation of lysine 9 of histone H3 is a mark for DNA

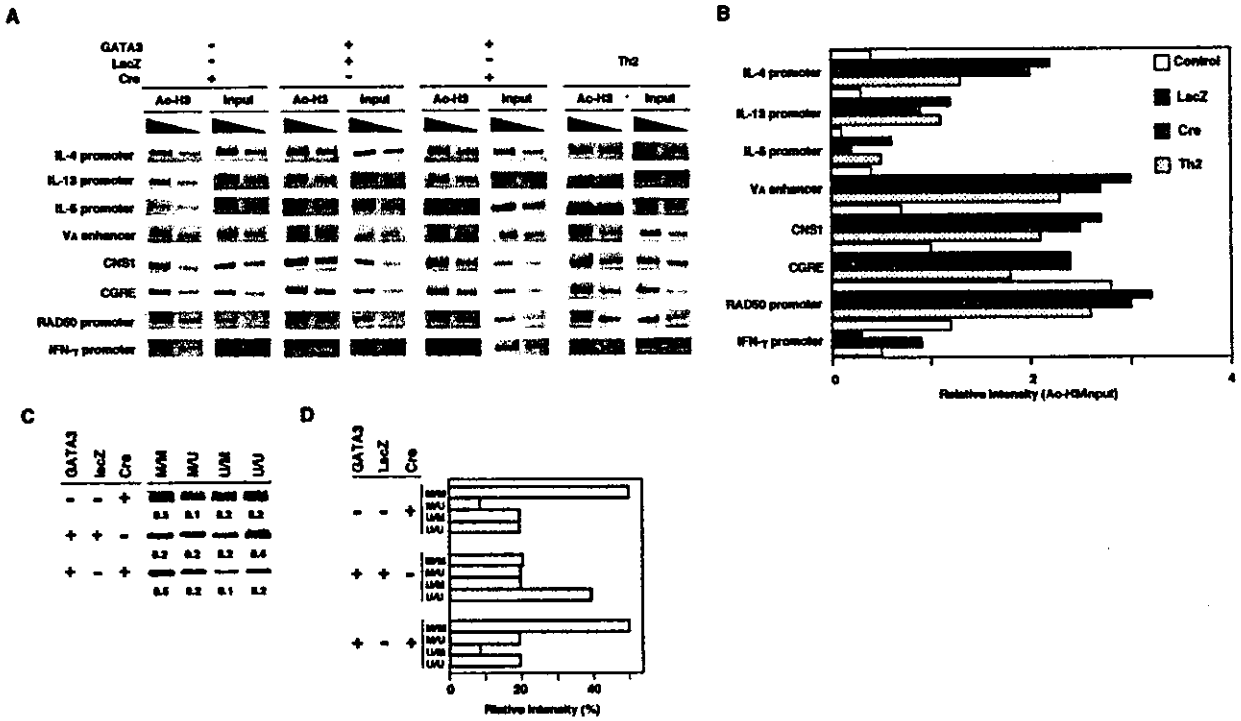

FIG. 6. **The role for GATA3 in the maintenance of open chromatin at the Th2 cytokine gene loci.** *A*, the acetylation status of histone H3 in nucleosomes associated with the Th2 cytokine gene loci was determined by ChIP assay. An Ad-LacZ vector was used as a control for Ad-Cre. Histone hyperacetylation of IL-4-, IL-13-, and IL-5-associated nucleosomes (IL-4 promoter, IL-13 promoter, IL-5 promoter, V_A enhancer, CNS1 and GATA3 response element) in Th2 cells after depletion of the GATA3 transgene prepared as in Fig. 4*A* was examined. The levels of acetylation in 5-day *in vitro* differentiated Th2 cells are also shown for comparison. Three independent experiments were done with similar results. *B*, the relative intensity of histone hyperacetylation (Ac-H3/Input DNA for the higher concentration bands) in each group shown in *panel A*. *C*, the DNA methylation status of the IL-4 intron 2 region assessed by a methylation-specific PCR technique. We focused on two cytidine residues within the IL-4 intron 2 region, and four patterns (both methylated, *M/M*; one methylated and one demethylated, *M/U* or *U/M*; and both demethylated, *U/U*) were detected. Three independent experiments were done with similar results. *D*, relative intensity (%) of each band shown in *panel C*.

methylation in *Neurospora crassa* (41). Also very recently, a tight correlation between methylation of lysine 9 of histone H3 and DNA methylation was reported in mammalian cells (42). Finally, it has been reported in many systems that there is an inverse correlation between acetylation and methylation of histone H3 lysine 9 in chromatin activation (43–45). Thus, it is likely that GATA3 is required solely for selective targeting of the histone acetyltransferase complex to the Th2 cytokine gene loci, and that this causes the appearance of demethylation indirectly. Whereas Hutchins *et al.* (46) reported that GATA3 is not required for the induction of DNA demethylation of intron 2 of the IL-4 gene locus, we detected demethylation of one site in the same intron 2 region by ectopic expression of GATA3 (Fig. 6). The reason for this apparent discrepancy is not clear, but it is possible that the PCR detection system we used here, to assess demethylation at specific sites in the IL-4 intron 2 region, may be more sensitive than the Southern blotting method used by Hutchins *et al.* (46).

In Fig. 4, the levels of residual GATA3 after Cre introduction appeared to be about 10% of control. However, the numbers of IL-4 or IL-5 producing cells and the levels of actual cytokine production were only reduced 2–3-fold (Fig. 5, *A* and *B*). These results may suggest that a certain low level of GATA3 protein is enough to maintain Th2 cytokine gene expression in some cells. It is also possible that the Th2 phenotype is already fixed in certain numbers of Th2 cells, in which unknown GATA3-independent mechanisms control the maintenance of the Th2 phenotype.

Murphy and colleagues (13) reported that the expression of GATA3 is controlled by autoactivation. Two distinct promoters control the expression of GATA3 (47). A newly identified promoter is suggested to be responsible for GATA3-dependent GATA3 transcription (GATA3 autoactivation). Thus, we performed Northern blot analysis to assess endogenous GATA3 levels, and could not detect any endogenous GATA3 after deletion of the *loxP*-flanked GATA3 transgene.[2] One possible explanation is that the expression level of GATA3 after *in vitro* site-specific recombination was too low to activate a GATA3-dependent promoter. In any event, the effect of deletion of the GATA3 transgene could not have been complicated in any way by the expression of endogenous GATA3 protein that might have been induced by so called autoactivation, as there was no endogenous GATA3 expression.

In our Cre/LoxP-based site-specific recombination system, the retrovirus-introduced transgene was deleted from the genome quite efficiently by adenovirus-mediated Cre introduction (Fig. 3, *A* and *B*). Thus, this system has proven to be a powerful tool for studying stage-specific roles of GATA3, and may be useful in this regard with various factors that are crucial for T cell activation, differentiation, and function. In summary, we demonstrated an important role for GATA3 in the maintenance of Th2 cytokine production, and remodeled

[2] M. Yamashita, M. Ukai-Tadenuma, T. Miyamoto, K. Sugaya, H. Hosokawa, A. Hasegawa, M. Kimura, M. Taniguchi, J. DeGregori, and T. Nakayama, unpublished observation.

open chromatin at the specific Th2 cytokine gene loci using a newly established *in vitro* site-specific recombination system.

Acknowledgment—We are grateful to Dr. Pandelakis A. Koni (Medical college of Georgia) for helpful comments and constructive criticisms in the preparation of the manuscript.

REFERENCES

1. Mosmann, T. R., and Coffman, R. L. (1989) *Annu. Rev. Immunol.* **7**, 145–173
2. Abbas, A. K., Murphy, K. M., and Sher, A. (1996) *Nature* **383**, 787–793
3. Constant, S. L., and Bottomly, K. (1997) *Annu. Rev. Immunol.* **15**, 297–322
4. O'Garra, A. (2000) *Nature* **404**, 719–720
5. Seder, R. A., and Paul, W. E. (1994) *Annu. Rev. Immunol.* **12**, 635–673
6. Reiner, S. L., and Locksley, R. M. (1995) *Annu. Rev. Immunol.* **13**, 151–177
7. Nelms, K., Keegan, A. D., Zamorano, J., Ryan, J. J., and Paul, W. E. (1999) *Annu. Rev. Immunol.* **17**, 701–738
8. Murphy, K. M., Ouyang, W., Farrar, J. D., Yang, J., Ranganath, S., Asnagli, H., Afkarian, M., and Murphy, T. L. (2000) *Annu. Rev. Immunol.* **18**, 451–494
9. Dent, A. L., Hu-Li, J., Paul, W. E., and Staudt, L. M. (1998) *Proc. Natl. Acad. Sci. U. S. A.* **95**, 13823–13828
10. Kaplan, M. H., Wurster, A. L., Smiley, S. T., and Grusby, M. J. (1999) *J. Immunol.* **163**, 6536–6540
11. Finkelman, F. D., Morris, S. C., Orekhova, T., Mori, M., Donaldson, D., Reiner, S. L., Reilly, N. L., Schopf, L., and Urban, J. F., Jr. (2000) *J. Immunol.* **164**, 2303–2310
12. Jankovic, D., Kullberg, M. C., Noben-Trauth, N., Caspar, P., Paul, W. E., and Sher, A. (2000) *J. Immunol.* **164**, 3047–3055
13. Ouyang, W., Lohning, M., Gao, Z., Assenmacher, M., Ranganath, S., Radbruch, A., and Murphy, K. M. (2000) *Immunity* **12**, 27–37
14. Agarwal, S., and Rao, A. (1998) *Curr. Opin. Immunol.* **10**, 345–352
15. Rengarajan, J., Szabo, S. J., and Glimcher, L. H. (2000) *Immunol. Today* **21**, 479–483
16. Zhang, D. H., Cohn, L., Ray, P., Bottomly, K., and Ray, A. (1997) *J. Biol. Chem.* **272**, 21597–21603
17. Zheng, W., and Flavell, R. A. (1997) *Cell* **89**, 587–596
18. Ouyang, W., Ranganath, S. H., Weindel, K., Bhattacharya, D., Murphy, T. L., Sha, W. C., and Murphy, K. M. (1998) *Immunity* **9**, 745–755
19. Lee, H. J., Takemoto, N., Kurata, H., Kamogawa, Y., Miyatake, S., O'Garra, A., and Arai, N. (2000) *J. Exp. Med.* **192**, 105–115
20. Farrar, J. D., Ouyang, W., Lohning, M., Assenmacher, M., Radbruch, A., Kanagawa, O., and Murphy, K. M. (2001) *J. Exp. Med.* **193**, 643–650
21. Bird, J. J., Brown, D. R., Mullen, A. C., Moskowitz, N. H., Mahowald, M. A., Sider, J. R., Gajewski, T. F., Wang, C. R., and Reiner, S. L. (1998) *Immunity* **9**, 229–237
22. Takemoto, N., Kamogawa, Y., Jun Lee, H., Kurata, H., Arai, K. I., O'Garra, A., Arai, N., and Miyatake, S. (2000) *J. Immunol.* **165**, 6687–6691
23. Yamashita, M., Ukai-Tadenuma, M., Kimura, M., Omori, M., Inami, M., Taniguchi, M., and Nakayama, T. (2002) *J. Biol. Chem.* **277**, 42399–42408
24. Avni, O., Lee, D., Macian, F., Szabo, S. J., Glimcher, L. H., and Rao, A. (2002) *Nat. Immunol.* **3**, 643–651
25. Fields, P. E., Kim, S. T., and Flavell, R. A. (2002) *J. Immunol.* **169**, 647–650
26. Takeda, K., Tanaka, T., Shi, W., Matsumoto, M., Minami, M., Kashiwamura, S., Nakanishi, K., Yoshida, N., Kishimoto, T., and Akira, S. (1996) *Nature* **380**, 627–630
27. Wan, Y. Y., Leon, R. P., Marks, R., Cham, C. M., Schaack, J., Gajewski, T. F., and DeGregori, J. (2000) *Proc. Natl. Acad. Sci. U. S. A.* **97**, 13784–13789
28. Nakayama, T., June, C. H., Munitz, T. I., Sheard, M., McCarthy, S. A., Sharrow, S. O., Samelson, L. E., and Singer, A. (1990) *Science* **249**, 1558–1561
29. Yamashita, M., Kimura, M., Kubo, M., Shimizu, C., Tada, T., Perlmutter, R. M., and Nakayama, T. (1999) *Proc. Natl. Acad. Sci. U. S. A.* **96**, 1024–1029
30. Omori, M., Yamashita, M., Inami, M., Ukai-Tadenuma, M., Kimura, M., Nigo, Y., Hosokawa, H., Hasegawa, A., Taniguchi, M., and Nakayama, T. (2003) *Immunity* **19**, 281–294
31. Nosaka, T., Kawashima, T., Misawa, K., Ikuta, K., Mui, A. L., and Kitamura, T. (1999) *EMBO J.* **18**, 4754–4765
32. Kimura, M., Koseki, Y., Yamashita, M., Watanabe, N., Shimizu, C., Katsumoto, T., Kitamura, T., Taniguchi, M., Koseki, H., and Nakayama, T. (2001) *Immunity* **15**, 275–287
33. Kanegae, Y., Takamori, K., Sato, Y., Lee, G., Nakai, M., and Saito, I. (1996) *Gene (Amst.)* **181**, 207–212
34. Guo, L., Hu-Li, J., Zhu, J., Watson, C. J., Difilippantonio, M. J., Pannetier, C., and Paul, W. E. (2002) *Proc. Natl. Acad. Sci. U. S. A.* **99**, 10623–10628
35. Kishikawa, H., Sun, J., Choi, A., Miaw, S. C., and Ho, I. C. (2001) *J. Immunol.* **167**, 4414–4420
36. Lavenu-Bombled, C., Trainor, C. D., Makeh, I., Romeo, P. H., and Max-Audit, I. (2002) *J. Biol. Chem.* **277**, 18313–18321
37. Kouzarides, T. (2002) *Curr. Opin. Genet. Dev.* **12**, 198–209
38. Nishioka, K., Chuikov, S., Sarma, K., Erdjument-Bromage, H., Allis, C. D., Tempst, P., and Reinberg, D. (2002) *Genes Dev.* **16**, 479–489
39. Zegerman, P., Canas, B., Pappin, D., and Kouzarides, T. (2002) *J. Biol. Chem.* **277**, 11621–11624
40. Inami, M., Yamashita, M., Tenda, Y., Hasegawa, A., Kimura, M., Hashimoto, K., Seki, N., Taniguchi, M., and Nakayama, T. (March 23, 2004) *J. Biol. Chem.* 10.1074/jbc.M401248200
41. Tamaru, H., Zhang, X., McMillen, D., Singh, P. B., Nakayama, J., Grewal, S. I., Allis, C. D., Cheng, X., and Selker, E. U. (2003) *Nat. Genet.* **34**, 75–79
42. Lehnertz, B., Ueda, Y., Derijck, A. A., Braunschweig, U., Perez-Burgos, L., Kubicek, S., Chen, T., Li, E., Jenuwein, T., and Peters, A. H. (2003) *Curr. Biol.* **13**, 1192–1200
43. Grewal, S. I., and Moazed, D. (2003) *Science* **301**, 798–802
44. Goll, M. G., and Bestor, T. H. (2002) *Genes Dev.* **16**, 1739–1742
45. Lachner, M., and Jenuwein, T. (2002) *Curr. Opin. Cell Biol.* **14**, 286–298
46. Hutchins, A. S., Mullen, A. C., Lee, H. W., Sykes, K. J., High, F. A., Hendrich, B. D., Bird, A. P., and Reiner, S. L. (2002) *Mol. Cell* **10**, 81–91
47. Asnagli, H., Afkarian, M., and Murphy, K. M. (2002) *J. Immunol.* **168**, 4268–4271

THE JOURNAL OF BIOLOGICAL CHEMISTRY
Vol. 279, No. 38, Issue of September 17, pp. 39454–39464, 2004
Printed in U.S.A.

Interleukin (IL)-4-independent Maintenance of Histone Modification of the IL-4 Gene Loci in Memory Th2 Cells*[S]

Received for publication, May 28, 2004, and in revised form, July 14, 2004
Published, JBC Papers in Press, July 16, 2004, DOI 10.1074/jbc.M405989200

Masakatsu Yamashita, Ryo Shinnakasu, Yukiko Nigo, Motoko Kimura, Akihiro Hasegawa, Masaru Taniguchi‡, and Toshinori Nakayama§

From the Department of Immunology, Graduate School of Medicine, Chiba University, 1-8-1 Inohana Chuo-ku, Chiba 260-8670 and the ‡Laboratory for Immune Regulation, RIKEN Research Center for Allergy and Immunology, Yokohama, 230-0045, Japan

Interleukin (IL)-4-induced STAT6 activation and the subsequent up-regulation of GATA3 are crucial for the induction of chromatin remodeling of the Th2 cytokine gene loci as Th2 cells undergo development. This study probes the role of these molecules in the maintenance of memory Th2 cells. IL-4 was not required to maintain the capability for Th2 cytokine production in *in vivo* generated antigen-specific memory Th2 cells. Histone H3-K9/14 hyperacetylation and intergenic transcripts associated with the *IL-4* gene locus were preserved in the absence of IL-4, but those associated with the *IL-13* gene were partially IL-4-dependent. Histone H3-K4 methylation of the *IL-13* and *IL-4* gene loci was fully preserved in memory Th2 cells and accompanied by memory cell-specific accumulation of Pol II complex to highly restricted sites. Thus, memory Th2 cells maintain a unique Th2-specific remodeled chromatin in the *IL-4* and *IL-13* gene loci by active molecular events that are IL-4-independent.

After TCR[1] recognition of antigens, naïve CD4 T cells differentiate into two distinct helper T (Th) cell subsets, Th1 and Th2 cells (1). Th1 cells produce IFNγ, and direct cell-mediated immunity against intracellular pathogens. Th2 cells produce IL-4, IL-5, and IL-13, and are involved in humoral immunity and allergic reactions. The direction of Th cell differentiation depends on the cytokine environment (2, 3). Naïve CD4 T cells stimulated with antigens in the presence of IL-12 differentiate into Th1 cells, whereas IL-4 drives differentiation into Th2 cells (4–6). The IL-12-mediated activation of signal transducer and activator of transcription (STAT) 4 is crucial for Th1 cell differentiation, while IL-4-mediated STAT6 activation is for Th2 cell development (7–9). In addition to the cytokines mentioned above, TCR stimulation by antigens also influences the direction of Th1/Th2 cell differentiation. We reported that efficient TCR-mediated activation of the $p56^{lck}$, calcineurin, and Ras-ERK MAPK signaling cascade was required for Th2 cell differentiation (10–12).

Recently, several transcription factors that control Th2 cell differentiation were identified (13, 14). Among them, GATA3 appears to be a master transcription factor for Th2 cell differentiation. GATA3 is selectively expressed in Th2 cells, and its ectopic expression induces Th2 cell differentiation even in the absence of STAT6 (15–18).

Changes in the chromatin structure of the Th2 cytokine (*IL-4/IL-5/IL-13*) gene loci occur during Th2 cell differentiation (19, 20). Recent studies have demonstrated that covalent modifications of histones play critical roles in epigenetic regulation (21). Recently, we and others (22–24) demonstrated that histone hyperacetylation of the Th2 cytokine gene loci occurs in developing Th2 cells in a Th2-specific and STAT6-dependent manner. Also, we demonstrated an essential role for GATA3 in Th2-specific histone hyperacetylation (22). We generated a precise map of the Th2-specific histone hyperacetylation within the type 2 cytokine gene loci, and identified a 71-bp conserved GATA3 response element (CGRE) at 1.6-kbp upstream of the *IL-13* locus exon 1. The CGRE appears to play a crucial role for GATA3-mediated targeting and downstream spreading of core histone hyperacetylation within the *IL-13* and *IL-4* gene loci in developing Th2 cells and Tc2 cells (22, 25).

Histone lysine methylation is considered to be a key epigenetic regulator (26). Methylation of specific lysine residues of histones is required for the maintenance of large, functionally distinct chromatin domains, such as heterochromatin correlated with histone H3 lysine 9 (H3-K9) (27). In contrast, transcriptionally active euchromatin preferentially contains methylated histones at H3-K36, H3-K79, and H3-K4 sites (28). Particularly, methylation at H3-K4 correlates well with active or permissive state of transcription (29). Furthermore, yeast Set1 (H3-K4 methyl-transferase) and Set2 (H3-K36 methyl-transferase) induce histone lysine methylation and functionally interact with RNA polymerase II (Pol II), suggesting that histone methylation at H3-K4 and H3-K36 is a hallmark of actively transcribed chromatin (26).

Some of the differentiated Th2 cells survive and are main-

* This work was supported by grants from the Ministry of Education, Culture, Sports, Science, and Technology (Japan) (Grants-in-aid of Scientific Research, Priority Areas Research 13218016; Scientific Research B 14370107, Advanced and Innovational Research program in Life Science and Special Coordination Funds), the Ministry of Health, Labor and Welfare (Japan) (a grant-in-aid for Research on Advanced Medical Technology), the Program for Promotion of Fundamental Studies in Health Science of the Organization for Pharmaceutical Safety and Research (Japan), the Human Frontier Science Program Research Grant (RG00168/2000-M206), and the Hamaguchi Foundation and Uehara Memorial Foundation. The costs of publication of this article were defrayed in part by the payment of page charges. This article must therefore be hereby marked "*advertisement*" in accordance with 18 U.S.C. Section 1734 solely to indicate this fact.

[S] The on-line version of this article (available at http://www.jbc.org) contains Supplementary Data.

§ To whom correspondence should be addressed: Dept. of Immunology, Graduate School of Medicine, Chiba University, 1-8-1 Inohana, Chuo-ku, Chiba 260 Japan. Tel.: 81-43-226-2200; Fax: 81-43-227-1498; E-mail: tnakayama@faculty.chiba-u.jp.

[1] The abbreviations used are: TCR, T cell antigen receptor; Th2, type-2 helper T; CGRE, conserved GATA3 response element; STAT, signal transducer and activator of transcription, CAR, Coxsackie/adenovirus receptor; EGFP, enhanced green fluorescence protein; HAT, histone acetyl transferase; ChIP, chromatin immunoprecipitation; STAT6-KO, STAT6-deficient; IL, interleukin; FITC, fluorescein isothiocyanate; Pol II, polymerase II; mAb, monoclonal antibody; WT, wild type; ELISA, enzyme-linked immunosorbent assay; IFN, interferon.

tained as memory Th2 cells for a long period *in vivo* (30, 31). Memory CD4 T cells can be generated from effector cells and can survive in the absence of MHC antigens (32, 33). The expression of either TCR (34) or Src-family kinases, $p56^{lck}$ and $p59^{fyn}$ appears not to be essential for the long-term survival (35). Also CD4 T cell survival is not directly linked to MHC-induced TCR signaling (36). In class II-restricted TCR transgenic mice lacking expression of the common cytokine receptor γ-chain (γc), the survival of naïve T cells is substantially impaired but memory T cell survival is apparently normal, suggesting that γc-dependent cytokines (IL-2, IL-4, IL-7, IL-9, and IL-15) is not required for memory CD4 T cell survival (37). As for homeostatic proliferation of CD4 memory T cells, IL-7 and IL-15 are not essential (33). Thus, in contrast to CD8 memory T cells, CD4 memory cells may not require any specific cytokine signals for their homeostatic maintenance (38, 39). Very recently, however, regulatory roles of IL-7 in the generation and survival of memory CD4 T cells were reported (40, 41). In addition, signals through the TCR as well as the IL-7 receptor appear to regulate the homeostasis of CD4 memory T cells (42). Th1 memory cells appear to be generated efficiently from an IFNγ non-producing population (43). Thus, it is still unclear whether any specific signals including those triggered by cytokines are required for the maintenance of memory Th2 cells. Furthermore, the molecular mechanisms that underlie the maintenance of capacity for Th2 cytokine production in memory Th2 cells, particularly those that preserve the Th2-specific remodeled chromatin are not fully understood.

In the present study, we used an adoptive transfer technique for the generation of antigen-specific memory Th2 cells *in vivo* to investigate the molecular events governing the maintenance of their Th2-specific cytokine production. In freshly prepared *in vivo* generated memory Th2 cells, histones associated with the *IL-4* and *IL-13* gene loci were hyperacetylated (at H3-K9/14) and di- and tri-methylated (at H3-K4), and these events were seen IL-4-deficient situation as well. Intergenic transcripts accompanied by highly localized accumulation of Pol II to CNS1, *IL-4* promoter, and V_A enhancer sites were observed. Thus, Th2-specific remodeled chromatin of the *IL-13* and *IL-4* gene loci is maintained in memory Th2 cells by active molecular events that are IL-4-independent.

EXPERIMENTAL PROCEDURES

Mice—BALB/c and BALB/c *nu/nu* mice were purchased from Clea Inc., Tokyo, Japan. IL4-deficient mice (44) and OVA-specific TCRαβ transgenic (DO.11.10 Tg) mice (45) were maintained under SPF conditions. All mice used in this study were maintained under specific pathogen-free conditions. Animal care was in accordance with the guidelines of Chiba University.

Reagents—The reagents used in this study are as follows: Fluorescein isothiocyanate (FITC)-conjugated anti-CD4 mAb (GK1.5-FITC), anti-CD62L mAb (MEL-14), anti-CD25 mAb (7D4), anti-CD69 mAb (H1.2F3), phycoerythrin (PE)-conjugated anti-CD4 mAb (GK1.5-PE), anti-CD44 mAb (IM7-PE), anti-CD122 mAb (TM-b1), anti-CD124 mAb (mIL-4R-M1), anti-CD127 mAb (4G3), and anti-CD132 mAb (TUGm2) were purchased from BD PharMingen, San Diego, CA. Anti-FcRgII and III mAb (2.4G2) and unconjugated anti-IL-4 mAb (11B11) were used as culture supernatants. Recombinant mouse IL-12 was purchased from BD PharMingen and recombinant mouse IL-4 was from TOYOBO, Osaka, Japan. The OVA peptide (residues 323–339; ISQAVHAA-HAEINEAGR) was synthesized by BEX Corporation, Tokyo, Japan.

The Generation of Effector and Memory Th1/Th2 Cells—Splenic CD4 T cells from DO11.10 OVA-specific TCR transgenic (Tg) mice were stimulated with an OVA peptide (Loh15, 1 μg/ml) plus APC under Th1- or Th2-skewed conditions for 5 days *in vitro* (10). We used these cells as effector Th1 or Th2 cells, respectively. The effector Th1/Th2 cells (3×10^7) were transferred intravenously into normal syngeneic BALB/c or BALB/c *nu/nu* recipient mice. In most of the experiments, 4 weeks after the cell transfer, $KJ1^+$ cells in the spleen were sorted by FACSVantage™ (BD PharMingen), and used as memory Th1and Th2 cells.

Cell Cycle Analysis—Splenic $KJ1^+$ cells were isolated by auto-MACS (Militenyi Biotec) with yielding purity >95%. The cells were fixed with 70% ethanol for 12 h, treated with RNase for 10 min at 37 °C and then suspended in 50 μg/ml PI (propidium iodide) solution. DNA contents were analyzed by flow cytometry.

Detection of Cell Division—Memory Th2 cells were prepared by sorting 4 weeks after cell transfer, and were labeled with CFSE (carboxyfluorescein diacetate succinimidyl ester, Molecular Probes) as described previously (46). Labeled cells were stimulated with OVA peptide (0.1 or 1 μM) plus APC for 16 h, and then subjected to flow cytometry.

ELISA—Cytokine production was assessed by ELISA as described (25).

Chromatin Immunoprecipitation (ChIP) Assay—Acetylation status of histone H3-K9/K4 was assessed using histone H3 (K9/14) ChIP assay kits (17-245; Upstate Biotechnology) and specific primers described in supplemental data. The ChIP assay for di- or tri-methylated histone H3-K4 was performed using anti-histone H3 di-methyl K4 antiserum (07–030; Upstate Biotechnology) and anti-histone H3 trimethyl K4 antiserum (ab7766; Abcam). The ChIP assay for GATA3, Pol II, and TFIIB was done as described (22). An anti-RNA polymerase II antiserum (C-21) and anti-TIFIIB (C-18) anti-serum was purchased from Santa Cruz Biotechnology (Santa Cruz, CA).

RT-PCR—RT-PCR analyses for GATA3, GATA3a, GATA3b, cytokines, β-actin, and intergenic regions of IL-13 and IL-4 were done as described (25).

Immunoblot Analysis—Immunoblot analyses for GATA3 and tubulin-α were done as described (25).

RESULTS

Generation of Antigen-specific Memory Th2 Cells in Vivo—We first established an experimental system where antigen-specific memory Th2 cells are generated and maintained efficiently *in vivo*. Splenic CD4 T cells from DO11.10 OVA-specific TCR transgenic (Tg) mice were stimulated with an OVA peptide (Loh15) plus APC under Th2-skewed conditions for 5 days *in vitro*, and then transferred intravenously into normal syngeneic BALB/c or BALB/c *nu/nu* recipient mice. The transferred DO11.10 Tg T cells were monitored by staining with the clonotypic KJ1 mAb. Typical staining patterns and the percentages of $KJ1^+$ cells/$CD4^+$ cells in BALB/c recipient mice are shown in Fig. 1*A*. A week after transfer, ~25% of splenic CD4 T cells were KJ1-positive. The numbers of $KJ1^+$ cells decreased at ~10% at the 2 week time point, and this level was maintained for at least for 16 weeks. Similar kinetics was observed in BALB/c *nu/nu* recipient mice (data not shown). A typical KJ1/CD4 staining pattern of spleen cells of BALB/c *nu/nu* recipient mice at 4 weeks after cell transfer, and DNA contents of the recovered $KJ1^+$ $CD4^+$ cells are shown in Fig. 1*B*. The PI staining profiles of the recovered $KJ1^+$ $CD4^+$ cells were indistinguishable from those of freshly isolated $KJ1^+$ cells from DO11.10 Tg mice, and almost all $KJ1^+$ cells were in G_0/G_1 phase.

Memory T cells proliferate rapidly in response to a low concentration of antigens as compared with naïve T cells (47). *In vivo* generated $KJ1^+$ memory Th2 cells in BALB/c *nu/nu* mice at the 4 week time point were purified by cell sorting (<98%), labeled with CFSE, and stimulated with two different doses of OVA peptides and APC for 16 h. Cell division analysis by flow cytometry showed that freshly isolated CD4 T cells from DO11.10 Tg mice did not proliferate during the first 16 h after stimulation, whereas substantial numbers of memory Th2 cells divided once in response to the antigenic peptide (27.4% for 0.1 μM and 37.9% for 1 μM OVA peptides) (Fig. 1*C*).

Next we assessed the expression levels of cell surface molecules including activation and memory markers and cytokine receptors on the freshly isolated memory Th2 cells (Fig. 1*D*). The expression levels of IL-4 receptor (R)α and common γ (cγ) chains were slightly higher in memory Th2 cells compared with those of freshly isolated $KJ1^+$ cells from DO11.10 Tg mice. Dramatically increased levels of IL-2Rβ and IL-7Rα chains were observed in memory Th2 cells. The activation markers, CD69 and CD25 (IL-2Rα chain), were not significantly ex-